# Characterization of NaA-coated ceramic membranes using pervaporation

N. N. Mzinyane

*I dedicate this dissertation to my beautiful daughter*
*Ntokozo Mzinyane*

# Characterization of NaA-zeolite membranes using pervaporation

**Nozipho Nompumelelo Mzinyane**

B.Sc. and B.Sc. Hons (University of the North)

**November 2005**

Dissertation submitted in fulfillment of the requirements of the degree

Magister Scientiae

at the North-West University

**Supervisor: Prof. H.M. Krieg**

**Co-supervisor: Prof. S. Marx**

# SUMMARY

Pervaporation has gained increasing attention as an energy saving process for separating azeotropes such as ethanol and water mixtures. Pervaporation distinguishes itself from other membrane processes in that it entails a phase transition step that occurs during the diffusion through the membrane, from the liquid phase in the feed to a vapor phase in the permeate. Pervaporation performance is mainly regulated by the physicochemical structure of the membrane rather than the vapor-liquid equilibrium of the system. A significant amount of literature is available to show the successful developments in terms of membranes and their use for pervaporation applications.

In spite of the substantial progress in pervaporation using polymeric membranes, as has been reviewed in several articles, zeolite membranes have various advantages over polymeric membranes, most notably their chemical and thermal stability. Due to their uniform molecular-sized pores, zeolites are highly suitable for the separation of molecules in mixtures both through their adsorption capacity and molecular sieving effects. It was the aim of this study to evaluate the suitability of our in-house manufactured centrifugally casted ceramic support for coating with a thin defect free NaA zeolite layer. The composite membrane was used to optimise some of the variables pertaining to water ethanol pervaporation.

Both single and double coated NaA ceramic composite membranes were manufactured. The integrity of the zeolite layer was confirmed by SEM. XRD was used to show that the coated layer consisted of the zeolite NaA. According to the XRD no impurities were present.

Both the single and double coated membranes were used for pervaporation. During pervaporation, the influence of the feed temperature and composition on both the single components and binary mixtures was determined. The binary mixtures were evaluated by varying the feed composition from 5 to 95% water and the feed temperature from 308K to 328K.

The single coated membrane performed better than the double coated membrane both in terms of flux and selectivity. The single coated membrane yielded a maximum flux of 4.50 $kg.m^{-2}h^{-1}$ at a selectivity of nearly 20 000, compared to the highest flux for the double coated membrane of 0.70 $kg.m^{-2}.h^{-1}$ and a selectivity of 4000. While the fluxes for the single components were higher than for the binary mixtures, the real selectivity for the binary mixture increased substantially from the ideal selectivity obtained with the single components. This was explained in terms of the preferential adsorption and condensation of water in the hydrophilic zeolite pores (both intra- and intercrystalline). Due to the condensation of water in the pores, the permeation of the ethanol is restricted, resulting in the significant separation factor obtained.

For the binary mixture, it was found that both the total flux and the water flux increase with increasing temperature and water content in the feed. The best compromise in terms of flux and selectivity, i.e. an average flux and maximum selectivity was obtained between 55 and 75% water in the feed at 328K. The high selectivity obtained throughout this study confirmed that a defect free zeolite NaA had been grown onto the smooth inside surface of the tubular ceramic support. The zeolite layer was furthermore very thin, confirmed by the high fluxes obtained compared to literature.

# OPSOMMING

Pervaporasie kry toenemend aandag as 'n energiebesparingsproses vir die skeiding van aseotrope soos byvoorbeeld etanol-en-water-mengsels. Pervaporasie verskil van ander membraanprosesse deurdat 'n fase-oorgang, van 'n vloeistoffase in die voerstroom na 'n dampfase in die permeaat, plaasvind tydens die diffusie deur die membraan. Pervaporasie word hoofsaaklik deur die fisies-chemiese struktuur van die membraan bepaal eerder as die damp-vloeistof ewewig van die sisteem. 'n Genoegsame hoeveelheid literatuur is beskikbaar om die suksesvolle ontwikkelinge in terme van membrane en hulle gebruik vir pervaporasie aan te dui.

Ten spyte van die substansiele vordering getoon in pervaporasie deur die gebruik van polimeriese membrane, waarvan in verskeie artikels 'n oorsig gegee is, het seolietmembrane verskeie voordele bo polimeriese membrane, waarvan hul chemiese en termiese stabiliteit die belangrikste is. As gevolg van hulle eenvormige porieë van molekulêre grootte, is seoliete uiters geskik vir die skeiding van molekules in mengsels, beide as gevolg van hulle adsorpsie-vermoë en hulle molekulêre siftingseffekte. Dit was die doel van hierdie studie om die geskiktheid van die self-vervaardigde, deur sentrifugering gegote keramiek ondersteuner te ondersoek vir die bedekking met 'n dun defek-vrye NaA-seolietlaag. Die saamgestelde membraan is gebruik om die veranderlikes wat van belang is vir die pervaporasie van water en etanol te optimeer.

Beide enkel- en dubbelbedekte saamgestelde NaA-keramiekmembrane is vervaardig. Die integriteit van die seolietlaag is bevestig deur SEM. XRD is gebruik om te wys dat die deklaag wel uit die seoliet NaA bestaan het. Volgens die XRD was daar geen onsuiwerhede teenwoordig nie.

Beide enkel- en dubbelbedekte membrane is vir pervaporasie gebruik. Tydens die pervaporasie is die invloed van die voertemperatuur en samestelling op beide enkelkomponente en binêre mengsels bepaal. Die binêre mengsels is ondersoek deur die samestelling van 5 tot 95% water en die voertemperatuur van 308K tot 328K te varieer.

Die enkelbedekte membraan het beter vertoon as die dubbelbedekte membraan beide in terme van fluks en selektiwiteit. Die enkelbedekte membraan het 'n maksimum fluks van 4.50 $kg.m^{-2}.h^{-1}$ teen 'n selektiwiteit van amper 20 000 vergeleke met die hoogste fluks verkry met die dubbelbedekte membraan wat 0.70 $kg.m^{-2}.h^{-1}$ was teen 'n selektiwiteit van 4000. Terwyl die fluks vir die enkel-komponente hoër was as vir die binêre mengsels, het die werklike selektiwiteit verkry met 'n binêre sisteem beduidend toegeneem teenoor die ideale selektiwiteit verkry met die enkel komponente. Dit is verklaar in terme van die voorkeur adsorpsie en kondensasie van die water in die hidrofiele seolietporieë. (beide intra- en interkristallyn). As gevolg van die kondensasie van water in die porieë, is die permeasie van die etanol beperk, wat aanleiding gegee het tot die hoë skeidingsfaktor wat verkry is.

By die binêre mengsel is gevind dat beide die totale fluks en die waterfluks toeneem met toenemende temperatuur en waterinhoud in die voerstroom. Die beste kompromis ten opsigte van fluks en selektiwiteit, dit wil sê 'n middelmatige fluks en maksimum selektiwiteit is verkry tussen 55 en 75% water in die voer teen 328K. Die hoë selektiwiteit deurgaans in die studie behaal het bevestig dat 'n defek-vrye seoliet NaA op die gladde binneoppervlak van 'n buisvormige keramiekondersteuner gegroei is. Die seolietlaag was verder baie dun, soos bevestig kon word deur die hoë flukse verkry vergeleke met die literatuur.

# ACKNOWLEDGEMENTS


- Ngithanda ukubonga uNkulunkulu ngokuzibonakalisa ubukhulu bakhe kimina, ngiphinde ngimbonge ngokuba nami ezifundweni zami.

- Prof Henning Krieg for his guidance and help throughout this research. For his motivations and enthusiasm, and telling me the golden rule for research 'Patience'. And also for opening his door for me, for my academic and personal problems.

- Prof Sannet Marx for her guidance and sharing her experience on the subject of pervaporation.

- My colleagues in the Membrane group for their help and support.

- To my dear parents for their understanding with everything I went through this year. Mom and Dad you were right as always things did workout at the end. Love you both.

- Ooh to my beautiful girl, Ntokozo you are a blessing. Mommy loves you.

- To my friends thank you for listen to me complaining about the GC in the tearoom and the laughs we shared there, they made my stay in Potchefstroom memorable.

# TABLE OF CONTENTS



## CHAPTER 1: Introduction

# CHAPTER 2: Literature survey



# Chapter 3: Experimental

# Chapter 4: Results and discussion



# Chapter 5: Evaluation

# Appendix A: Gas chromatography

# Chapter 1 INTRODUCTION

## 1.1. Membranes

A membrane is a selective barrier between two phases. One approach to classify membranes is to differentiate between biological and synthetic membranes [1]. These two membrane types differ in structure and functionality. Biological membranes, such as liposomes and vesicles from phospholipids, are increasingly important in medicinal and biomedicinal separation processes, while synthetic membranes are mostly used in industrial separation processes.

Synthetic membranes can be subdivided into organic (polymeric or liquid) and inorganic (e.g. ceramic, metal, silica and zeolite) membranes. Inorganic membranes are more expensive than organic membranes, due to the cost of the materials and their synthesis process. Inorganic membranes, however, have the advantage of temperature stability, resistance towards solvents, well-defined stable pore structures and the possibility of sterilization. Organic membranes are generally limited to temperatures below 200 °C, while inorganic membranes can withstand temperatures up to 700 °C [1].

Synthetic membranes can also be classified according to their morphology or structure. The structure of synthetic membranes can either be symmetric or asymmetric. The two classes can be subdivided further as shown in Figure 1.1

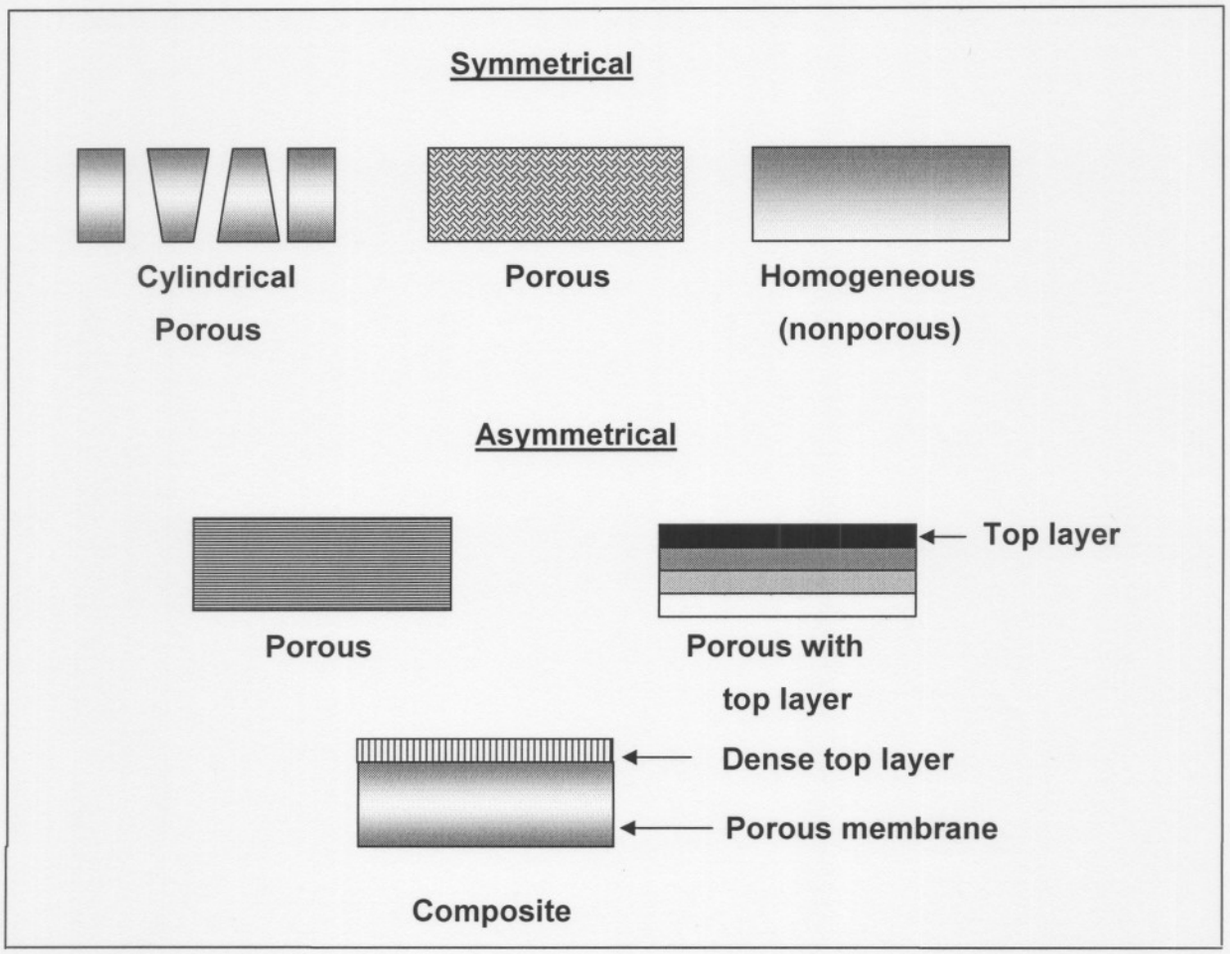


**Figure 1.1 Schematic representations of various membrane morphologies [1]**

### 1.1.1. Ceramics membranes

Ceramic membranes are increasingly being used in a broad range of industries such as the biotechnological, pharmaceutical and chemical industries. Ceramic membranes with a narrow pore size distribution have been developed that exhibit unique physical and chemical properties which give them significant advantages over polymeric and stainless steel membranes [2].

These advantages include better structural stability without the problem of swelling or compaction. Generally these types of membranes can withstand harsh chemical environments and high temperatures [3].

### 1.1.2. Zeolite Membranes

Zeolites are crystalline microporous materials with well-defined structures that contain aluminium, silicon and oxygen in a regular framework [4]. Zeolite membranes are formed when crystals grow on a surface (membrane support) and interlock to give a coherent layer [5]. Other applications of zeolites include catalysis, adsorption and ion-exchange [6].

Since the early 1990s, intensive research efforts have focussed on the development of zeolitic membranes [7]. In recent years there has been much interest in the preparation of zeolite membranes [9, 10], which can for example be employed for the removal of water from hydrocarbons [11]. The specific properties of zeolite membranes which have attracted the attention of scientists include:

- Long-term stability at high temperatures,
- resistance to harsh environments,
- resistance to high pressure drops,
- inertness to microbiological degradations, and
- easy cleanability and catalytic activation [8].

Zeolite membranes may be hydrophilic or hydrophobic, depending on their structure and chemical composition. Hydrophobicity and hydrophilicity of the zeolite is important for the selective adsorption in organic/water separations [12]. Hydrophilic membranes such as zeolite NaA have pores large enough for water molecules to pass but not organic molecules such as ethanol [13] and are thus suitable for separating water from organics. Hydrophobic silica zeolites and Ge-ZSM5 (germanium substituted MFI structure), on the other hand, preferentially

adsorb organic solvents. Zeolite NaA membranes are very sensitive to acidic environments and this prevents their use even under moderately low-pH applications (e.g. removal of water from esterification reactions). The stability of the zeolite in acid environments increases with its silica content resulting in a trade-off between hydrophilicity and acid stability [14].

## 1.2. Membrane Processes

There are many different membrane separation processes, such as gas separation (GS), vapour permeation (VP), pervaporation (PV), membrane distillation (MD) and membrane contactors (MC), based on different separation principles or mechanisms. In spite of these differences, all of these processes have one thing in common, the membrane. The membrane is at the heart of every one of these processes and can be considered to be a permselective barrier or interface between two phases. A schematic representation of a generalised membrane separation process is given in Figure 1.2.

Phase 1 (in Figure 1.2.) is the feed or upstream phase while Phase 2 is the permeate or downstream phase. Separation is achieved because one component from the feed mixture is preferentially transported across the membrane under a specific driving force. Possible driving forces include:

- Pressure difference ($\Delta P$),
- concentration difference ($\Delta C$),
- temperature difference ($\Delta T$), or
- electrical potential difference ($\Delta E$) [14].

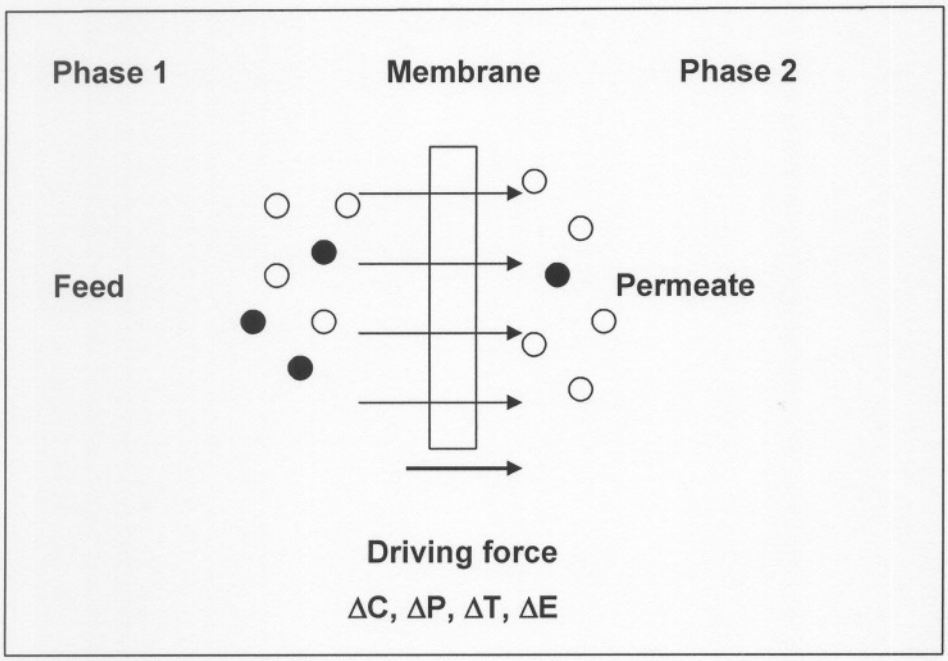


**Figure 1.2 Schematic representation of a two phase membrane separation system [1]**

The extent of the driving force is determined by the gradient in potential ($=\partial X/\partial x$), or approximately by the difference in potential across the membrane ($\Delta X$) divided by the membrane thickness ($\ell$), i.e. [1]

$$\text{Driving force} = \Delta X / \ell \text{ [N/mol]} \qquad (1.1)$$

### 1.2.1. Pervaporation

Kober first introduced the term pervaporation in 1917 by combining the words "permeation" and "evaporation" in a publication reporting selective permeation of water from aqueous solutions of albumin and toluene through collodion (cellulose nitrate) films [15].

However, the process did not come into commercial use until 1982 when the "Gesellschaft für Trenntechnick GmbH" (GFT) in Germany installed a pervaporation plant to separate water from concentrated alcohol solutions [16]. It was in 1988 when the first commercial scale plant was commissioned in Bethéniville, France, where pervaporation was applied to the dehydration of ethanol [17].

## 1.3. Aims and Objective

The goal of this project is to manufacture and evaluate the suitability of zeolite coated ceramic membranes for the selective removal of water from alcohol mixtures. While the water/ethanol azeotrope is difficult to separate by distillation, the azeotropic character of the mixture does not hamper the separation using pervaporation with zeolitic membranes. All membranes will be evaluated in terms of single solvents and various ratios of binary mixtures.

## 1.4. Outline of the thesis

Each chapter has a short introduction of the subject discussed. An overview of the most relevant literature on pervaporation and the basic concepts relevant to zeolite membranes and pervaporation are discussed in Chapter 2.

In Chapter 3, the experimental apparatus used and the experimental procedures are discussed. The evaluation of different membranes and the pervaporation performance of the zeolite NaA membranes in terms of pure water, pure ethanol and binary mixtures at different feed temperatures is given in Chapter 4. An evaluation of the project is presented in Chapter 5.

## 1.5. References


[1] M. Mulder, 1996, Basic principles of Membrane technology, The Netherlands, Kluwer academic Publishers, 2nd edition, 12, 210

[2] R. Sondhi, R. Bhave and G. Jung, 2003, Applications and benefits of ceramic membranes, Membrane Technology Volume 2003, 11, 5-8

[3] A.W. Verkerk, P. van Male, M.A.G. Vorstman and J.T.F. Keurentjies, 2001, Properties of high flux ceramic pervaporation membranes for dehydration of alcohol/water mixture, Separation and Purification Technology,. **22-23**, 689-695

[4] J.J. Jafar and P.M. Budd, 1997, Separation of alcohol/water mixtures by pervaporation through zeolite A membrane, Microporous Materials, **12**, 305-311

[5] K. T. Jung and Y.G. Shul, 2001, Preparation of ZSM-5 zeolite film and its formation mechanism, Journal of Membrane Science, **191**, 189-197

[6] A.S.T.Chiang, Lecture note for seminar at Chemistry Department NCU, November 1998

[7] F. Morón, M. P. Pina, E. Urriolabeitia, M. Menéndez, J. Santamaría, 2002 Preparation and characterization of Pd-zeolite composite membrane for hydrogen separation, Desalination, **147**, 425-431

[8] R. Broodryk, 2000, Preparation and application of zeolite membranes, Potchefstroom University for Christian Higher Education, MSc Thesis, 10

[9] A. Tavolaro, E. Drioli, 1999, Verified Syntheses of zeolite materials: Preparation of zeolite membranes, Advanced Materials, **11**, 975

[10] M.A. Salomon, J. Coronas, M. Menéndez and J. Santamaría, 2000, Synthesis of MTBE in zeolite membrane reactors, Applied Catalysis A General, **200**, 201-210

[11] T.C. Bowen, S. Li, V.A. Tuan, J. L. Falconer and R.D. Noble, 2002, Pervaporation of aqueous organic mixtures through Ge-ZSM-5 zeolite membranes, Desalination, **147**, 327-329

[12] M. Lassinanti, 2001, Synthesis, characterisation and properties of zeolite films and membranes, Luleá Tekniska University of Technology, Thesis, 3

[13] A. Navajas R. Mallada, C. Téllez, J. Coronas, M. Menéndez and J. Santamaría, 2002, Preparation of mordenite membranes for pervaporation of water-ethanol mixtures, Desalination, **148**, 25-29.

[14] L. Casado, R. Mallada, C. Téllez, J. Coronas, M. Menéndez and J. Santamaria, 2003, Preparation, characterization and pervaporation performance of mordenite membranes, Journal of Membrane Science, **216,** 135-147

[15] R.Y.M. Huang, 1991, Elsevier Science Publishers B.V., Pervaporation membrane separation process, Chapter 1, 1-62

[16] S. Thomas, A. Resch and L. Voelz, 1998, Pervaporation History, 1

[17] L. Malherbe, 2000, Potchefstroom University for Christian Higher Education, Application of pervaporation for the selective removal of water from an esterification reaction-mixture, MSc Dissertation, 6

# Chapter 2 LITERATURE SURVEY

## 2.1. Introduction

Membrane technology represents an effective and energy-saving alternative separation process. The most important membrane processes are microfiltration (MF), reverse osmosis (RO), ultrafiltration (UF), electrodialysis (ED), gas separation (GS) and pervaporation (PV). The use of pervaporation for the separation of organic liquid mixtures, especially ethanol-water systems, has experienced growing acceptance over the past years [1].

Pervaporation is considered an alternative method for the separation of liquid mixtures since the separation is not dependent on vapour-liquid equilibrium for separation. In the last 20 years, pervaporation has been widely studied both in academia and industry [2]. Compared to traditional technologies, such as distillation and adsorption, pervaporation offers many advantages such as:

- high separation efficiency
- low energy consumption and
- simple operation [2].

The process is even more attractive for separating azeotropic mixtures since the separation is not based on the relative volatility of the components in the mixture, but rather on the relative affinity of the components for the membrane [3]. Both organic and inorganic membranes have been used for pervaporation.

## 2.2. Pervaporation

Pervaporation is a membrane process used for the separation of liquid mixtures which are difficult (or impossible) to separate by conventional methods. During pervaporation, the liquid feed mixture is kept in contact with the membrane on the feed or upstream side at atmospheric pressure, while the permeate is continuously removed as vapour due to a low vapour pressure existing on the permeate or downstream side. This low (partial) vapour pressure is achieved using a carrier gas or vacuum pump as is illustrated in Figure 2.1[4].

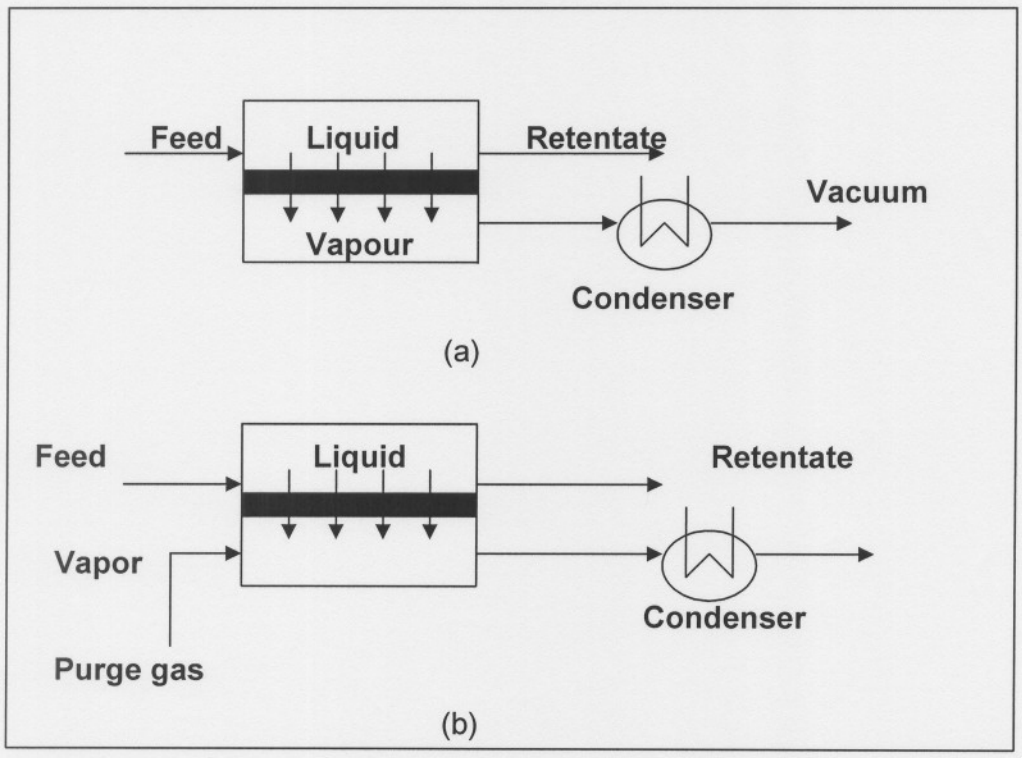


**Figure 2.1 Schematic diagrams of (a) a vacuum pervaporation (b) and an inert purge pervaporation process**

Vacuum pervaporation, which is customarily referred to as standard pervaporation, is the most widely used, while carrier gas pervaporation is normally of interest if the permeate can be discharged without condensation. An advantage of carrier gas

pervaporation is that no vacuum is necessary which lowers the cost [5]. However, minimal total energy consumption is clearly obtained for vacuum compared to sweep gas operations [6].

The effectiveness of a membrane in separating most components including liquid mixtures is characterized by two parameters, flux and selectivity (for example separation factor). Flux is expressed as the amount of permeate collected per unit time per unit membrane area either as mass flux ($kg.m^{-2}.h^{-1}$), mole flux ($mol.m^{-2}.h^{-1}$) or volume flux ($m^3.m^{-2}.h^{-1}$ or $L.m^{-2}.h^{-1}$). Selectivity of the permeation process to a particular solute in pervaporation is expressed in terms of the fractions of each component in the feed and permeate. This selectivity can be calculated by means of

$$\alpha_{a/b} = \left( \frac{Y_a / Y_b}{X_a / X_b} \right) \qquad (2.1)$$

where α is the separation factor, $Y_a$, $Y_b$ and $X_a$, $X_b$ are the weight fractions of the solute a and b in the permeate and the feed respectively.

## 2.3. The effect of operational conditions on pervaporation performance

The two main keys in pervaporation, as in any membrane process, i.e. membrane selectivity and flux, depend on a range of variables including:

- temperature,
- permeate pressure (vacuum),
- feed composition and
- membrane properties.

It is important to understand the effects of these factors so that the proper operating conditions and membranes can be selected for the separation of a particular mixture [7]. While the experimental section of this study deals with inorganic membranes, mostly organic membranes are discussed in this literature section which was due to the expansive amount of literature on organic membranes compared to inorganic membranes. Reference to inorganic membranes is made where available.

### 2.3.1. Temperature

Temperature affects the transport of components in the liquid feed and the membrane in that both mass transfer coefficient of the components in the liquid phase and sorption of components into the membrane increase with the feed temperature [8]. While the temperature of the feed increases, the flux increases according to the Arrhenius law:

$$\ln J = \ln J_0 - \frac{Ep}{RT} \qquad (2.4)$$

where J is the permeate flux ($mol.m^{-2}.h^{-1}$) and $J_o$ is the pre-exponential factor, $E_p$ ($kJ.mol^{-1}$) is the apparent activation energy for permeation, R ($kJ.mol^{-1}.K^{-1}$) is the gas constant and T(K) is the absolute temperature.

The selectivity is strongly dependant on temperature, where a decrease in selectivity is observed with increasing temperature [9]. According to the free volume theory, an increase in temperature can increase the thermal motion of the polymer chains and generate more free volume in the polymer matrix to facilitate absorption and diffusion of permeate in an organic membrane. The increase in the free volume makes the membrane more permeable but less discriminative to the permeation of the permeating components, which leads to a higher permeation rate and a lower separation factor [10].

### 2.3.2. Permeate pressure (vacuum)

One of the most important process parameters is the permeate pressure, which, together with the operating temperature, determines the driving force for the process [11]. Since the permeate pressure is directly related to the activity of the components at the downstream side of the membrane, the permeate pressure strongly influences the pervaporation characteristics [12, 13]. In general, the driving force will decrease, resulting in a lower flux as the downstream pressure increases [9].

The change in permeate pressure also affects the selectivity. However, the selectivity can increase or decrease with increasing permeate pressure, depending on the relative volatility of the permeating components [8].

Another effect that determines the effective permeate pressure, is the porosity of the membrane support. Since the membrane flux is partially determined by the local pressure at the surface of the membrane, a pressure drop over the porous support will lead to smaller activity gradients of the components in the active membrane, resulting in a deterioration of pervaporation characteristics, especially for asymmetric and composite membranes [8].

### 2.3.3. Feed composition

The feed composition is yet another very important factor in determining pervaporation flux and selectivity. Since all the components in the feed mixture affect liquid sorption, membrane swelling and diffusion, the permeation rate of a particular component is affected by all other components present [14]. In a two-component feed mixture for example, one of the components interacts more strongly with the membrane, resulting in membrane swelling. As the concentration of this component increases, the membrane swells more and the flux increases. Diffusivities of both components increase with membrane swelling and

pervaporation selectivity decreases. Thus, for a given membrane and liquid mixture, the total pervaporation flux increases monotonically with the concentration of the more permeating component in the feed, while selectivity decreases [15].

### 2.3.4. Membrane properties

The choice of the membrane is very important since the efficiency of pervaporation depends greatly on the membrane used. Consequently, much of the current research and developments in the field of membrane technology are therefore aimed at developing membranes that yield high fluxes at high selectivities [16]. Two basic membrane types, organic and inorganic, are usually distinguished. These two types will be discussed in more detail in section 2.4 and 2.5 respectively.

A very important membrane property is its thickness. Flux is generally inversely proportional to the membrane thickness when the membrane is kept under a low downstream pressure and if the diffusion of the permeating species through the membrane is the rate determining step of the transport [17]. This suggests that a thin membrane yields high fluxes. Deviation from this simple relationship may be observed if the downstream pressure is increased. If this pressure approaches the saturated vapour pressure of the permeate, desorption slows down and may become rate limiting.

In the case of a composite membrane, the situation is more complex. The behaviour of the membrane greatly depends on its orientation with respect to the permeate flow. Generally, the highest selectivity is observed when the dense selective layer faces the feed mixture. On the other hand, the reverse orientation yields a higher permeation flux.

The use of very thin membranes in pervaporation deserves special consideration. As the diffusion resistance of the membrane decreases, a downstream boundary resistance to permeate transfer can become relevant [17]. This would result in a

higher than vapour-phase equilibrium loading of the permeate at the interface of the membrane. Furthermore, the enhanced flux, as the result of the very thin membrane, can make it increasingly difficult to maintain low permeate pressure and control concentration polarisation [17].

### 2.4. Membrane manufacturing

Composite membranes usually consist of a support and one or two top layers. Therefore, it is important that the support structure is suitable for the coating of the top layers, which should be defect free and as thin as possible. The requirements for the support are a high permeability and smooth and regular surface on which the top layer can be coated. Surface roughness, defects and irregular pore-size distributions can cause defects and irregular structure in the top layer. There are two methods which can be used for support manufacturing, the first is the extrusion where the defects and irregular packing are almost unavoidable and centrifugal casting where the distribution of particles in suspensions is much better and good packing can be achieved. Therefore, the porous structure of the support is regular and the surface smooth. Although centrifugal casting is slightly more expensive than extrusion it thus remains suitable for the manufacturing of high-quality tubes [31]

## 2.5. Additional considerations for polymeric membranes

Polymeric membranes have been widely used to separate numerous feed mixtures by pervaporation. However, polymeric membranes have some limitations in their application, due to insufficient thermal, mechanical, and chemical stability. This has led to novel developments in inorganic membranes [18] due to their higher chemical and thermal stability in comparison to organic membranes [4].

### 2.5.1. Coupling Effect

Membrane performance is defined in terms of the selectivity of the membrane and the permeation rate. The selectivity and the permeation rate are governed by the solubility and diffusivity of each component of the feed mixture within and through the membrane matrix. Prediction of the selectivity and diffusivity is often difficult because there is a coupling of individual component fluxes. Coupling of fluxes occurs when the transport of a certain component through the membrane is affected by the presence of one or more of the other components. This can occur in both the liquid phase and the polymer phase [22].

The coupling effect takes place due to the mutual interaction between the components and the polymer, which directly influences the permselectivity of the membrane [23]. Coupling phenomena are difficult to measure quantitatively and even more difficult to predict in relation to the separation properties [22].

## 2.6. Single and binary permeation

There are specific considerations which have to be kept in mind when working with single components or binary mixtures. These will be briefly elaborated on the following two sub-sections.

### 2.6.1. Single component permeation

In pervaporation, the vapor pressure at the permeate side or downstream from the membrane is much lower than the saturated pressure, which means that the activity a" (= $p_i/p^0$) is very low or almost zero. In the case of pure liquids, the activity on the upstream side is unity (a'=1), assuming that both interfaces of the membrane are in thermodynamic equilibrium with the upstream and the downstream phase (which means that the activity of the liquids in the feed is equal

to the activity just inside of the membrane). Accordingly, the activity in the membrane changes from a' equals 1 to a" approaching zero, going from the upstream side to the downstream side of the membrane [28].

### 2.6.2. Binary mixture permeation

The transport of mixtures through a polymeric membrane is generally more complex because the components of the mixture interact both with each other and with the membrane. Furthermore, in the case of a binary liquid mixture consisting of component 1 and 2, the flux can be described in terms of the solubility and diffusivity [29], which is different from single-component permeation, because solubility or diffusivity of one component in the mixture can and often is, influenced significantly by the presence of the other component or components. This was, for example, shown by the permeation results obtained by Huang and Lin, who found that all the components of the mixtures permeated considerably faster than either of the pure components for a benzene/ hexane/ polyethylene system [30].

Separation of binary gaseous (gas permeation, vapour permeation) or liquid (pervaporation) mixtures by dense membrane processes has already received considerable attention and has found numerous applications in the chemical, food and pharmaceutical industries [31].

## 2.7. Pervaporation by zeolite membranes

In recent years the use of zeolite membranes for pervaporation has attracted considerable attention and is probably the best known example of an inorganic membrane for pervaporation. Composite ceramic membranes (ceramic support coated with a zeolite active layer) do not have any of the swelling problems associated with polymer membranes. This makes them ideal candidates for application in separation by pervaporation or vapour permeation. NaA and silicate based membranes have been used extensively for the removal of organic compounds from water [24,25,26]. In general, hydrophilic zeolite membranes, for example zeolite NaA, have been used for the dehydration of organic solvents while hydrophobic zeolite membranes, for example silicalite, have been used for the removal of organics from water [27].

## 2.8. Conclusion

The most important advantages of pervaporation, compared to other separation methods (e.g. distillation and adsorption), is its low energy consumption and its ability to separate azeotropic mixtures. Furthermore, the required equipment (laboratory scale) is small, while the maintenance cost is low and the operation is simple.

The many studies that have been done using polymeric membranes to separate alcohol from water mixtures highlighted some of the shortcomings observed, such as the swelling of the organic (polymeric) membranes leading to higher permeabilities and lower selectivities. Inorganic membranes are ideal candidates for the separation by pervaporation because of their chemical and physical properties. However, most literature regarding zeolites has focussed on gas separation with comparatively less work having been done on pervaporation using these membranes.

## 2.9. References


[1] J.R. González-Velasco, J.A. González-Marcos, C. Lopez- Dehesa, 2002, Pervaporation of ethanol-water mixtures through poly(1-trimethylsily-1-propyne (PTMSP) membranes, Desalination, **140,** 61-65

[2] B. Han, C. Chen, R. Wickramasinghe, 2002, Computer simulation and optimisation of pervaporation process, Desalination, **145**, 187-192

[3] S. Marx, P. van der Gryp, H. Neomagus, R. Everson and K. Keizer, 2002, Pervaporation separation of methanol from methanol/tert-amyl methyl ether mixtures with a commercial membrane, Journal of Membrane Science, **209**, 353-362

[4] A. Arttiaga, E.D. Gorri, C. Casado and I. Oritiz, 2003, Pervaporative dehydration of industrial solvents using a zeolite NaA commercial membrane, Separation and Purification Technology, **32**, 207-213

[5] X. Feng and R.Y.M. Huang, 1997, Liquid separation by membrane pervaporation: A review, Industrial & Engineering Chemistry Research, **36**, 1048-1066

[6] C. Vallieres, E. Favre, X. Arnold and D. Roizard, 2003, Separation of binary mixtures by dense membrane processes: influence of inert gas entrance under variable downstream pressure conditions, Chemical Engineering Science, **58**, 2767-2775

[7] H. Shaban, 1996, Removal of water from aroma aqueous mixtures using pervaporation processes, Separation Technology, **6**, 69-75

[8] R. Jiraratananon, A. Chanachai, R.Y.M. Huang and D. Uttapap, 2002, Pervaporation dehydration of ethanol-water mixtures with chitosan/hydroxyethyl/cellulose (CS/HEC) composite membranes: I Effect of operational conditions, Journal of Membrane Science, **95**, 143-151

[9] B. Smitha, D. Suhanya, S. Sridhar and M. Ramakrishma, 2004, Separation of organic mixtures by pervaporation: A review, Journal of Membrane Science, **241**, 1-21

[10] P. Sampranpiboon, R. Jiraratanonon, D. Uttapap, X. Feng and R.Y.M. Huang, 2000, Pervaporation separation of ethyl butylrate and isopropanol with polyether block amide (PEBA) membranes, Journal of Membrane Science, **173,** 53-59

[11] J. Olsson and G. Tragardh, 2001, Pervaporation of volatile organic compounds from water: I influence of permeate pressure on selectivity, Journal of Membrane Science, **187**, 23-37

[12] R. Rautenbach and R. Albrecht, 1984, On the behaviour of asymmetric membranes in pervaporation, Journal of Membrane Science, **19**, 1, 1-22

[13] B. K. Dutta, W. Ji and Sikdar, 1997, Pervaporation: Principles and application, Separation and purification Methods, **25** (2), 225-226

[14] J.J. Jafar and P.M. Budd, 1997, Separation of alcohol/water mixtures by pervaporation through zeolite A membrane, Microporous Materials, **12**, 305-311

[15] C.Y. Chen, 2004, Carbon dioxide recovery by vacuum swing adsorption, Separation and Purification Technology, **39**, 51-65

[16] A. S. T. Chiang, November 1998, Lecture note for seminar at Chemistry Department, NCU

[17] P. van der Gryp, 2003, Potchefstroom University for Christian Higher Education, Separation by pervaporation of methanol from tertiary amyl methyl ether using a polymeric membrane, MSc Thesis, 29-30

[18] M. Kondo, M. Komori, H. Kita and K. Okamoto, 1997, Tubular-type pervaporation module with zeolite NaA membranes, Journal of Membrane Science, **133**, 133-141

[19] L. Malherbe, 2000, Potchefstroom University for Christian Higher Education, Application of pervaporation for the selective removal of water from an esterification reaction-mixture, MSc Thesis, 52

[20] W. Chuang, T. Young, D. Wang, R. Luo and Y. Sun, 2000, Swelling behavior of hydrophobic polymers in water/ethanol mixtures, Polymer, **41**, 8339-8347

[21] J.S. Yang, H.J. Kim, W.H. Jo and Y.S. Kang, 1998, Analysis of pervaporation methanol-MTBE mixtures through cellulose acetic and cellulose triacetate membranes, Polymer, **39**, 1381-1385

[22] K. Rachau, H. H. Schwarz, R. Apostel and D. Paul, 1996, Dehydration of organic by pervaporation with polyelectrolyte complex membranes: some considerations concerning the separation mechanism, Journal of Membrane Science, **113**, 31-41

[23] J. Smart, V. M. Starov, R. C Schucker and D. R Lloyd, 1998, Pervaporative extraction of volatile organic compounds from aqueous systems with use of tubular transverse flow module: Part II experimental results, Journal of Membrane Science, **143**, 159-179

[24] J. Ren and C. Jiang, 1998, The coupling effect of the thermodynamics swelling process in pervaporation, Journal of Membrane Science, **140,** 221-233

[25] D. Shah, K. Kissick, A. Ghorpade, R. Hannah and S. Bhattacharyya, 2003, Pervaporation of alcohol-water and dimethylformamide – water mixtures using hydrophilic zeolite NaA membranes: mechanisms and experimental results, Journal of Membrane Science, **215**, 235-247

[26] M. Kondo, M. Komori, H. Kita and K. Okamoto, 1997, Tubular-type pervaporation module with zeolite NaA membrane, Journal of Membrane Science, **133**, 133-141

[27] F. P. Cuperus and R.W. van Gemert, 2002, Dehydration using ceramic silica pervaporation membranes the influence of hydrodynamic conditions, Separation and Purification Technology, **27,** 225-229

[28] R.Y.M. Huang, 1991, Elsevier Science Publishers B.V., Pervaporation membrane separation process, Chapter 2, 166,228-229

[29] C. Vallieres, E. Favre, X. Arnold and D. Roizard, 2003, Separation of binary mixtures by dense membrane process: Influence of inert gas entrance under variable downstream pressure conditions, Chemical Engineering Science, **58**, 2767-2775

[30] G. Li, E. Kikuchi and M. Matsukata, 2003, A study on the pervaporation of water-acetic acid mixtures through ZSM-5 zeolite membrane, Journal of Membrane Science, **218,** 185-194

[31] S.J. Doong, W.S. Ho and R.P. Mastondrea, 1995, Prediction of flux and selectivity in pervaporation through a membrane, Journal of Membrane Science, **107**, 129-146

[31] G.C Steenkamp, H.W.J.P. Neomagus, H.M. Krieg, K. Keizer, Centrifugal casting of ceramic membrane tubes and the coating with chitosan, 2001, Separation and Purification Technology **25**, 407-413

# EXPERIMENTAL

Chapter 3

The experimental section of this study consists of two steps: the manufacture of the NaA-coated composite ceramic membrane and the characterization of the membrane by means of the pervaporation of a water/ethanol mixture.

## 3.1. Membrane manufacture

The NaA-coated tubular ceramic membranes used in this study were manufactured in-house. The manufacturing procedure for both the support and the zeolite NaA-membrane are presented below.

### 3.1.1. Ceramic support synthesis

#### 3.1.1.1. Materials

The $\alpha$-$Al_2O_3$ powder (AKP-15) used for the manufacture of the tube was obtained from Sumitomo Chemical Company Ltd., Japan. According to the supplier, AKP-15 has a particle size of 0.62 µm and a BET surface area of 3.5 $m^2.g^{-1}$. APMA (Ammonium PolyMethAcrylate aqueous solution) was obtained from Darvan C, R.T. Vanderbilt Company Inc., Norwalk, USA, while the $NH_4OH$ ammonium hydroxide was obtained from Labchem. Deionised water was used through-out the study.

### 3.1.1.2. Methods

For the manufacture of a 6cm support, 120g α-$Al_2O_3$ powder (AKP-15) was mixed with 10ml APMA and 600 ml deionised water. The mixture of powder, water and APMA had a total volume of 120 ml and was adjusted to a pH of 9.5 by adding 1.5 ml of $NH_4OH$.

The resulting suspension was ultrasonically treated for 15 minutes using a frequency of 20 kHz and a transducer output power of 100 W (Model 250 Sonifier, Branson Ultrasonics Corporation, Danbury, USA). With this suspension, tubes of 6 cm in length were prepared in a custom-built apparatus using steel moulds. Before pouring the suspension into the mould, the inside of the mould was coated with a solution of 4g Vaseline in 45g petroleum ether (boiling range 60-80°C) to ensure easy mould release. The mould was filled with the suspension and sealed with a lid and PTFE tape. The tubes were centrifuged for 20 minutes at 17.000 rpm after which the remaining liquid was decanted from the mould. The green tubes were dried horizontally in the mould for one day at 30°C to facilitate mould release. After drying, the green tubes were removed from the moulds and sintered horizontally for 1 hour on a flat surface at 1050°C with a heating and cooling rate of 1°C/min. After cooling, the edges of the support were smoothed with sandpaper and filed to the required length (± 5 cm). The support was sonicated twice for 5 minutes to remove all foreign particles. The support was dried in an electronically controlled hot-air oven for 12 hours at 120 $^0$C, and then allowed to cool down to room temperature. For the zeolite synthesis, the support was wrapped in Teflon tape. The inside surface of the support was firstly brushed and then dusted with $N_2$ gas to remove any remaining foreign particles [1].

### 3.1.1.3. Characterization

#### 3.1.1.3.1. Water permeability

The water permeability of the ceramic membrane support was determined using a permeation set-up consisting of an $N_2$ gas cylinder, a storage vessel and the permeation cell as shown in Figure 3.1.

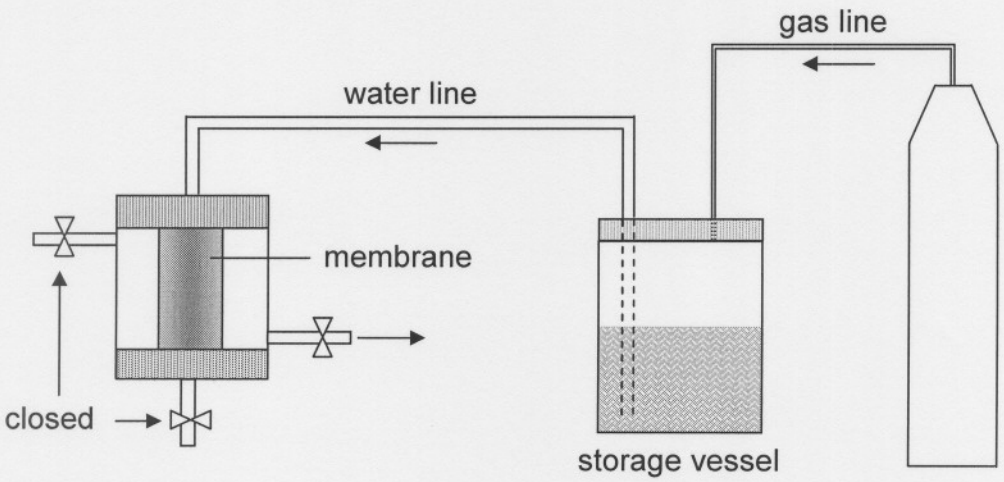


**Figure 3.1: Diagrammatic presentation of the water permeation set-up**

The nitrogen gas provides the driving force for the deionised water (feed) in the storage vessel. The outlet of the storage vessel was connected to the permeation cell in which the ceramic support was placed. The supports were sealed with two O-rings within the permeation cell. The permeation module has two inlets and two outlets so that the module can be used in dead-end mode as well as in cross-flow mode. However, for the permeation studies, the cell was only used in the dead-end mode, i.e. one inlet and one outlet remained closed. The volumetric flow rate was calculated at five different pressures from 0.2-1.0 MPa, from which the water permeability was calculated for each support. The mass of the permeate collected was measured with a balance [1].

#### 3.1.1.3.2. Mercury porosimetry and scanning electron microscopy (SEM)

Pore size and porosity of the support were determined using scanning mercury intrusion porosimetry (Autopore III, Micromeretics). The microstructure and morphology of the ceramic support were examined with SEM (Philips XL 30).

### 3.1.2. Hydrothermal synthesis of a zeolite NaA-membrane

#### 3.1.2.1. Materials

For the NaA synthesis, sodium metasilicate pentahydrate ($Na_2 SiO_3$. $5H_2O$ BDM), sodium aluminate (41% $Na_2O$, 54% $Al_2O_3$, Riedel-de Haën), sodium hydroxide (97%, Aldrich) and deionised water were used as nutrients in a molar oxide composition ratio of $48.9Na_2O:Al_2O_3:5.08SiO_2:979.2H_2O$. Polysulfone was purchased from Aldrich and chloroform (99%) was obtained from Saarchem.

#### 3.1.2.2. Methods

##### 3.1.2.2.1. Single–layer synthesis

For the preparation of the Al solution, 4.807g NaOH was weighed and added to 20g of $H_2O$. The mixture was stirred until all the NaOH had dissolved. Subsequently, 0.452 g $NaAlO_2$ was added and the mixture was stirred for another 60 min. To prepare the Si solution, 3.481g NaOH was weighed and was added 20g of $H_2O$. The mixture was stirred until all the NaOH had dissolved. Subsequently, 2.628g $Na_2SiO_3.5H_2O$ was added and stirred for another 60 min.
The $Al^{3+}$-containing solution was then added drop wise to the silicate mixture while stirring and the resulting clear solution was allowed to age for exactly 30 minutes at room temperature. 15ml of this solution was added drop wise to an autoclave containing a fitted Teflon tube and the prepared (Teflon-coated) ceramic support. The autoclave was rotated at room temperature for 30 minutes before the

synthesis at 358 K for 4 hours in an electronically controlled hot-air oven. The autoclave, whilst still rotating, was left to cool down to room temperature for 3 hours. The composite membrane was removed from the remaining solution, thoroughly rinsed with deionised water and extensively sonicated in deionised water over intervals of 10 minutes for 1 hour to remove any excessive or loosely bound zeolitic phases. Finally the membrane was dried inside a desiccator for 2 days.

#### 3.1.2.2.2. Double-layer synthesis

For a double-layer synthesis, a similar procedure as described above for the single-layer synthesis was used. However, the single-layered membrane was not dried prior to synthesis. Another difference from the single layer synthesis was that the aluminium-silicate solution was aged for 1 hour (instead of 30 minutes) before being added drop wise to the autoclave. Furthermore, once the autoclave had been loaded, it was immediately heated to 358K for 4 hours. After the synthesis and cooling the coated support was sonicated in deionised water three times for 6 minutes before being stored in deionised water.

### 3.1.2.3. Characterisation

The microstructure and morphology of the ceramic support and zeolite layer were examined with SEM (Philips XL 30). XRD analysis of the zeolite phase was performed on a Bruker-Nonius D5005 diffractometer with 1/4 circle eulerian cradle, using Ni-filtered $CuK_{\alpha}$-radiation, operating at 45 kV (tube voltage) and 25 mA (tube current). For the permeation, related characterisation pervaporation was used.

## 3.2. Pervaporation

### 3.2.1. Materials

The chemicals used for pervaporation include absolute ethanol (99.5%) and acetonitrile (99.8%) Both had been purchased from Merck Chemical Company. All reagents were used without further purification. Possible impurities present did not influence the experimental results, because a single distinct peak was observed during GC (gas chromatograph) analysis. Deionised water was used.

### 3.2.2. Methods

A standard pervaporation set-up with all the typical accessories required to conduct pervaporation experiments was build and used. A photo and a schematic diagram illustrating the experimental apparatus used in this study is presented in Figure 3.1 and Figure 3.2 respectively

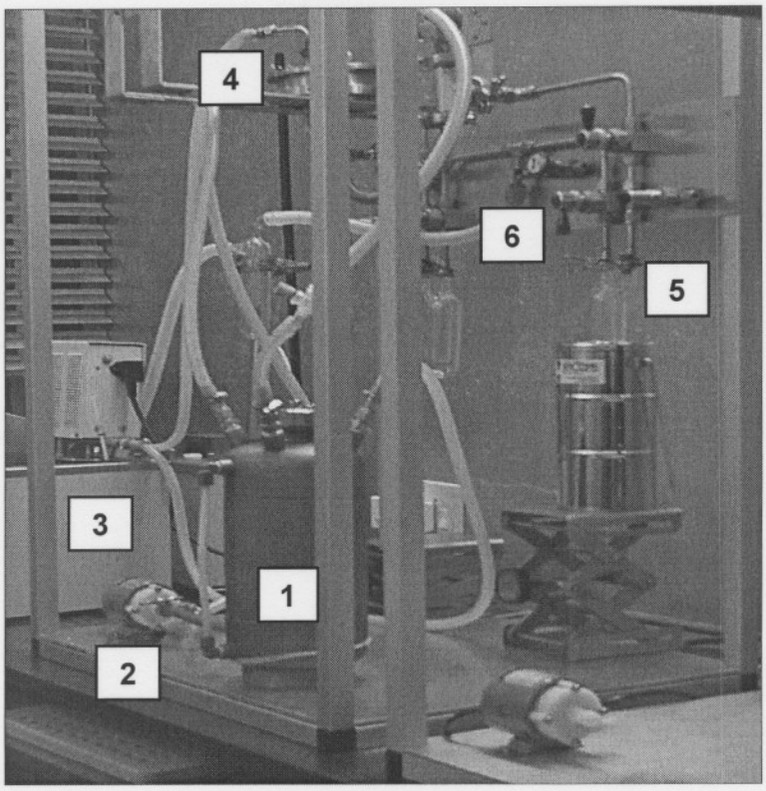


**Figure 3.2** **A photo of the experimental pervaporation set-up where 1 is the feed vessel, 2 the magnetic pump, 3 the water bath, 4 the membrane module, 5 the cold trap and 6 the vacuum line**

Warm water from the water bath (3) was circulated to the feed vessel (1) via a circulator to maintain the desired temperature in the feed vessel. The feed solution was fed directly to the membrane side of the membrane module (4) with a magnetic pump (2). The permeate side of the module/cell was kept at a constant pressure of 0.4 kPa using a vacuum (6) and the vapor from the permeate side was collected in cold traps filled with liquid nitrogen (5). The composition of the collected fluid in the cold trap and the feed was analysed using a Carlo Erbo GC 6000 Vega series 2 gas chromatograph [2].

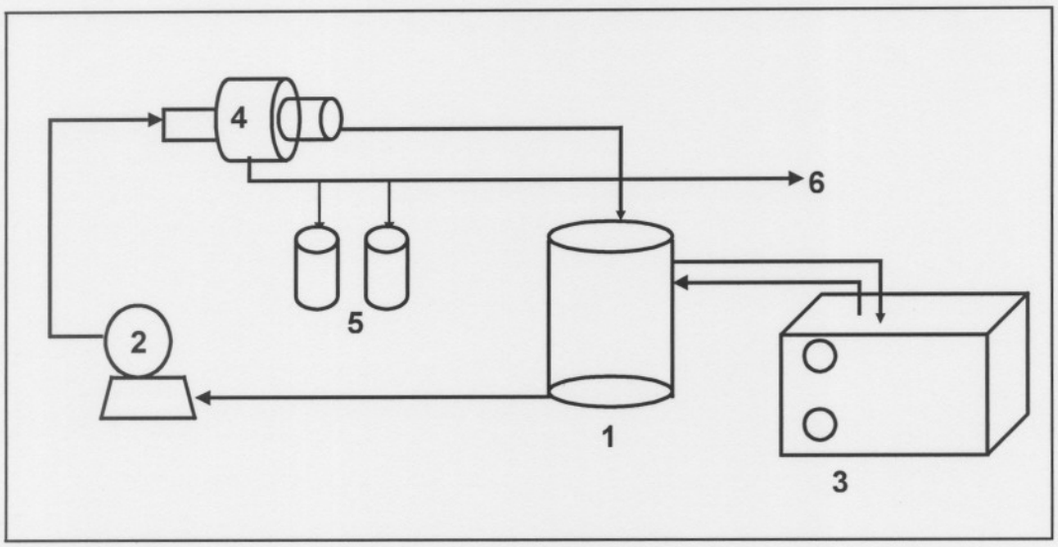


**Figure 3.3 Schematic diagram of the pervaporation apparatus 1 feed vessel, 2 magnetic pump, 3 water bath, 4 membrane module, 5 cold trap, 6 vacuum pump [2]**

Some of the equipment used for the pervaporation is presented in Table 4.1

**Table 4.1: Details of the equipment used for pervaporation**

| Equipment | Supplier/Type | Operating conditions |
|---|---|---|
| Feed vessel (1) | stainless steel tank | 2 L |
| Feed pump (2) | Iwaki magnetic pump (Iwaki Co Ltd, Japan) | 0.3 ± 0.001 $m^3$/h |
| Water bath (3) | 13L water bath with circulator (Labchem) | 35-55 °C |
| Vacuum pump (6) | Edwards, 2-stage high vacuum pump (Wirsam) | 0.01 bar |

### 3.2.3. Analysis

A Carlo Erbo GC 6000 Vega series 2 chromatograph with an FID was used. An HP-FFAP capillary column from J&W Scientific was used. Before the analysis of the permeate and the feed mixture, the GC was calibrated using standard solutions and these conditions:

- Inlet temperature: 220 $^0$C
- Detector temperature: 230 $^0$C
- Carrier gas: 5.1ml.min$^{-1}$
- Oven temperature: 90 $^0$C
- Retention time of ethanol: 1.4 min
- Retention time for Acetonitrile 1.6 min

For the GC, analysis 0.9g of a sample from the permeate was mixed with 0.1g acetonitrile which was added as an internal standard. The areas of the peaks, resulting from the analysis of the mixtures on the GC, were used to determine the composition of the solutions by converting the measured areas to mole fractions using the calibration curves which will be shown in detail in Appendix A. Each sample was analysed three times and the peaks were distinct with no overlapping.

### 3.2.4. Membrane module

To ensure a tight seal of the composite membrane within the membrane module, both ends of the composite membrane were sealed using a polysulfone polymer. To prepare the polymer solution 1g polysulfone was dissolved in 19g chloroform.
The ends (± 1cm) of the NaA-coated composite membrane were immersed twice (without drying in between) in the polysulfone solution to prevent them from leaking. The sealed membrane was dried overnight in a horizontal position at room temperature. After drying, the tubular membranes were placed into the membrane module. Viton O-rings were used to seal the membrane into the module as

demonstrated in Figure 3.4. Glass was used for the outer wall of the membrane module to make it easier to see what is happening to the membrane within the module. This was used to test for the presence of visible leaks in which case water or vapor would become visible.

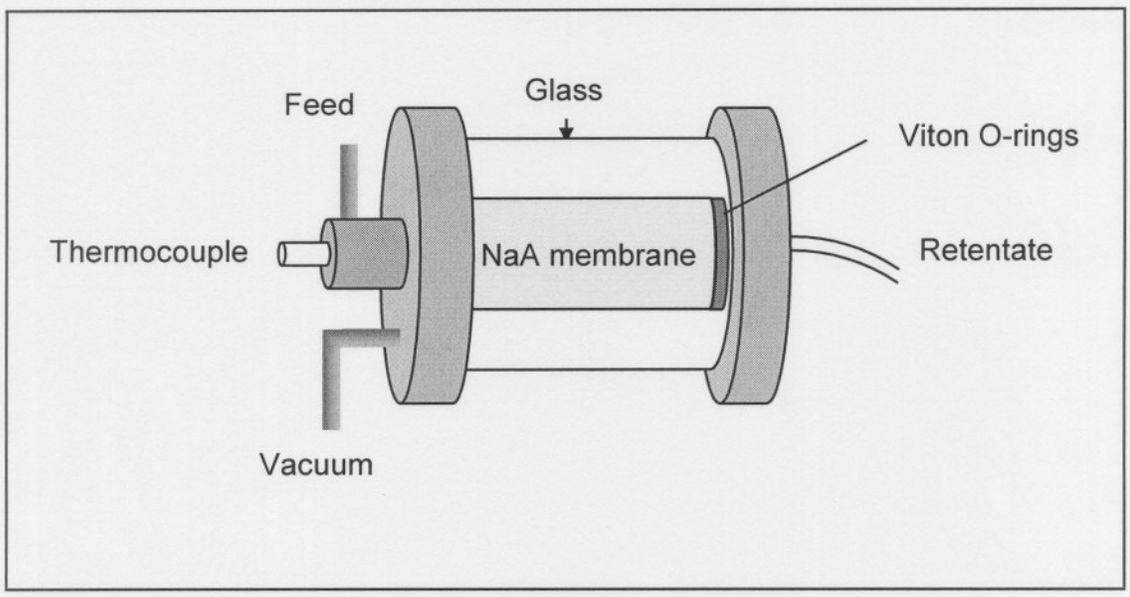


**Figure 3.4 A schematic diagram of a membrane module containing the NaA-composite membrane used for pervaporation**

### 3.2.5. Variables

The pervaporation experiments were performed using both single feed (water and ethanol) as well as binary mixtures of water/ethanol on single and double NaA-coated composite membranes. Various feed compositions and temperatures were investigated at a constant pressure of 0.4 kPa. For the binary study, the feed composition was varied between 5 and 95 % of water to study the effects of the feed composition on the pervaporation characteristics. The feed temperature was ranged between 35 $^{0}$C and 55 $^{0}$C to investigate the effect of temperature on pervaporation. Fifty five degrees Celsius was the limit to prevent the ethanol from boiling. The conditions that yielded the best results (selectivity) for the single

coated NaA-composite membranes were selected for the study on the double coated NaA-composite membrane.

## 3.3. References

[1] G.C Steenkamp, H.W.J.P. Neomagus, H.M. Krieg, K. Keizer, Centrifugal casting of ceramic membrane tubes and the coating with chitosan, 2001, Separation and Purification Technology **25**, 407-413

[2] S. Marx, 2002, Potchefstroom University for Christian Higher Education, Application of pervaporation to the separation of methanol from tertiary amyl methyl ether, Thesis,

# RESULTS AND DISCUSSION

# Chapter 4

## 4.1. Introduction

This chapter is divided into three sections, namely membrane characterization (Section 4.2), pervaporation (Section 4.3) and a comparison of the pervaporation results obtained in this study to the results presented in literature (Section 4.4).

## 4.2. Membrane characterization

### 4.2.1. Ceramic support

A ceramic support was successfully made by centrifugal casting. It was subsequently characterized by scanning electron microscopy (SEM), mercury extrusion and a water permeation study.

#### 4.2.1.1. Scanning electron microscopy (SEM)

The microstructure and morphology of the ceramic support was examined with a SEM (Philips XL 30). An image of the inner surface of a tubular support made from AKP-15 powder (particle size of 0.62 μm) is shown in Figure 4.1. The packing is regular and the surface is smooth. The smooth surface on the inside is a result of the centrifugal casting, which makes supports prepared by this method ideal for direct coatings with thin zeolite layers.

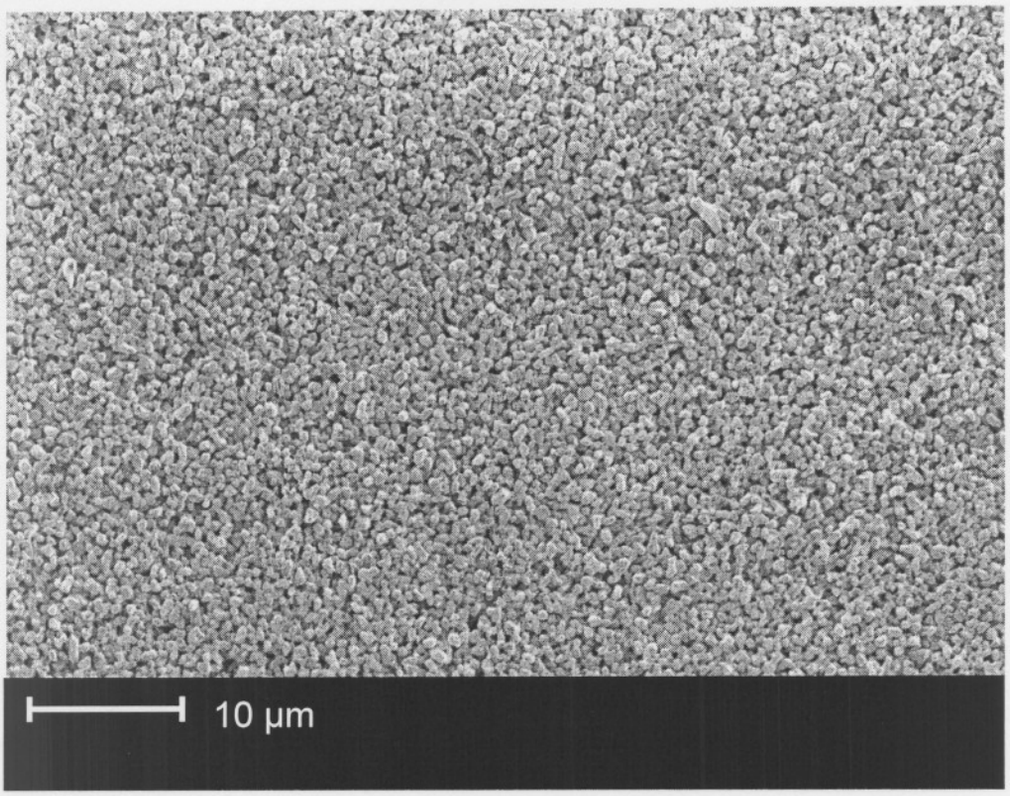


**Figure 4.1 SEM-micrograph of the inner surface of a centrifugally casted AKP-15 support sintered at 1050 $^{0}$C**

#### 4.2.1.2. Mercury porosimetry

A mercury porosimetry analysis was done on the alumina support to determine the porosity, pore size distribution and the average pore size of the support. According to the analysis, the support made from AKP-15 powder had a narrow pore size distribution with an average pore size of 0.26 µm. The calculated porosity was 37%.

#### 4.2.1.3. Water permeability

The water permeability of the support was determined by measuring the flux at different pressures. The permeability for the AKP-15 support, which was obtained

by calculating the slope of the flux versus pressure plot, is 41 $L.m^{-2}.h^{-1}.bar^{-1}$, which is in agreement with the value calculated using the extended Hagen-Poisseuille equation (4.1),

$$J = \frac{\varepsilon}{\tau} \frac{r^2}{8\eta} \frac{\Delta P}{\Delta x} \qquad (4.1)$$

where J is the water flux ($m.s^{-1}$), $\varepsilon$ the porosity (%), $\tau$ (-) the tortuosity (which is approximately 2.5 for a spherical particle packing), r the pore radius (m), $\eta$ the water viscosity ($10^{-3}$ Pa.s), $\Delta P$ the pressure difference (Pa) and x the membrane thickness (m) [1].

### 4.2.2. Zeolite NaA-coating

Having successfully made and characterised the ceramic support, the support was coated both with a single and double NaA-zeolite layer. The morphological properties of the zeolite layer was characterised by SEM and XRD. The transport properties were characterised by pervaporation.

#### 4.2.2.1. Scanning electron microscopy (SEM)

SEM-micrographs of a single and double coated NaA-zeolite membrane are shown in Figure 4.2 (a) and Figure 4.2 (b), respectively. The approximate thickness of the NaA-zeolite active layer was approximately 5 µm for the single coating and 10 µm for the double coating.

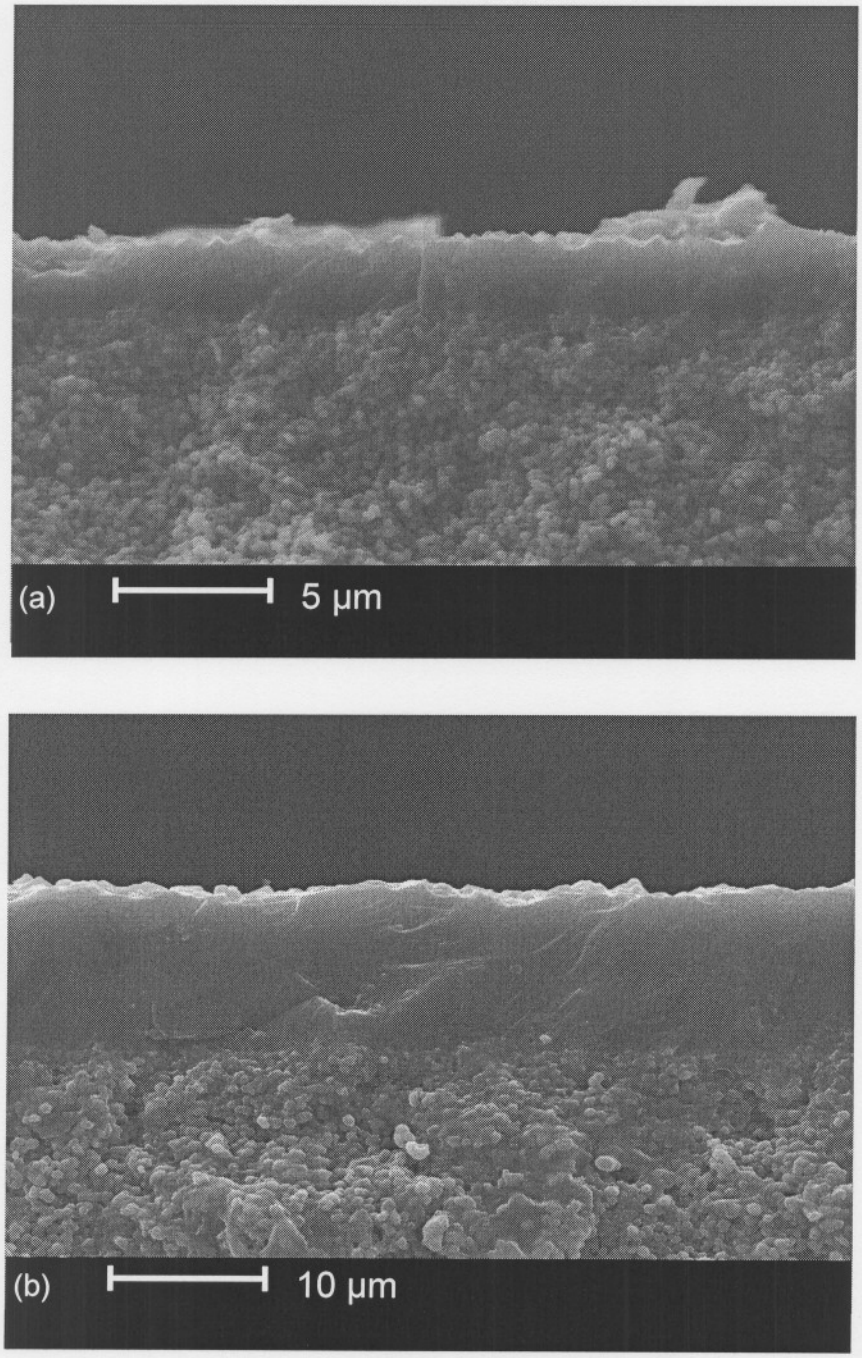


**Figure 4.2** **SEM-micrograph (cross-section) of a densely intergrown cubic zeolite NaA-crystal layer grown on an AKP-15 support surface where (a) has a single coating and (b) a double coating**

It is clear from Figure 4.2 that a defect free attachment of the zeolite on the ceramic support was achieved, both with the single and double coated zeolite composite membrane.

In Figure 4.3, a SEM-microgaph is shown of the surface of the NaA-monolayer of fully developed and densely intergrown crystals, 2-5 µm in size with the typical NaA-morphology.

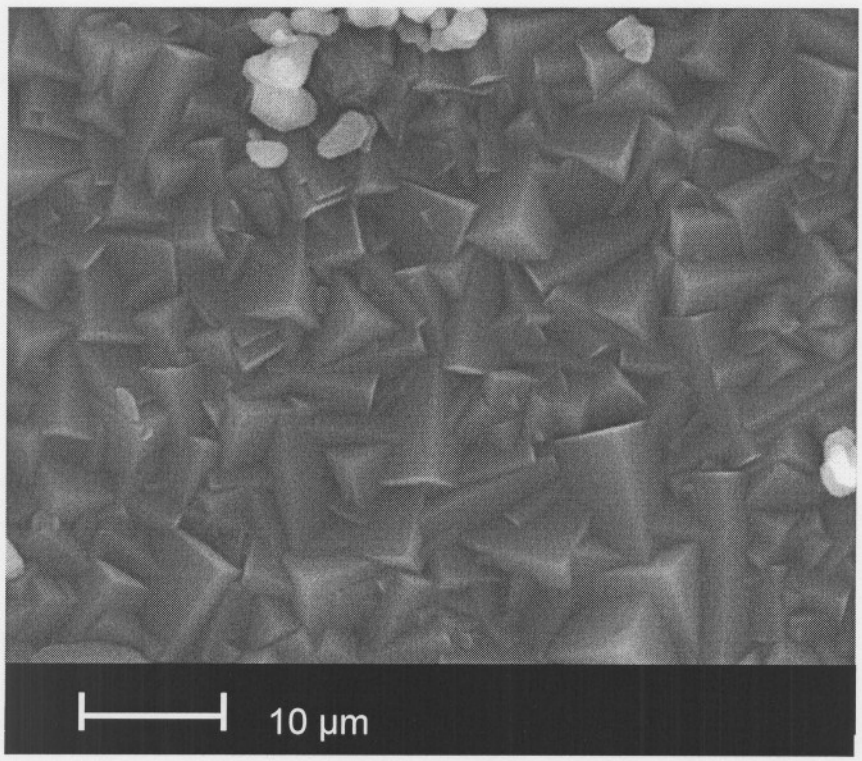


**Figure 4.3 SEM-micrograph of a densely intergrown cubic zeolite NaA-crystal layer grown on an AKP-15 support surface**

#### 4.2.2.2. X-Ray diffraction analysis (XRD)

An XRD analysis was carried out on the NaA-zeolite layer to confirm the crystal structure of the zeolite membrane. When comparing the obtained XRD pattern (Figure 4.4) to the simulated framework diffractogram for hydrated zeolite LTA [2], it

is clear that the manufactured zeolite layer consists solely of NaA, i.e. no other crystalline impurities were present according to the obtained XRD pattern.

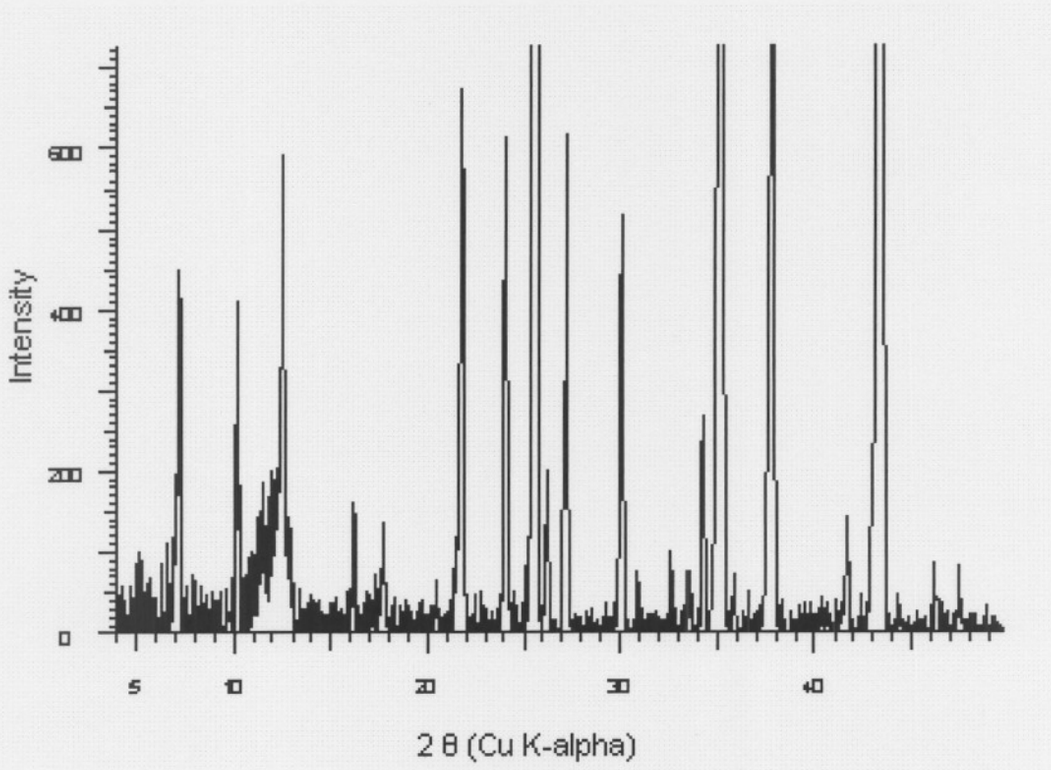


**Figure 4.4 XRD pattern of a double coated composite zeolite membrane**

The four peaks at 26, 35, 38 and 43 are indicative reflections from the α- $Al_2O_3$ support.

## 4.3. Pervaporation

In this section, the pervaporation results of the zeolite NaA-membrane using ethanol and water as well as binary mixtures of ethanol and water are presented. The influence of the feed composition and feed temperature on permeation was investigated by measuring the total flux and the selectivity through the membrane

as a function of these variables. A comparison is made between single and double coated zeolite membranes.

### 4.3.1. Single components

In Figure 4.5, a typical graph is presented of the raw data obtained from pervaporation, i.e. the mass of the permeate recovered from the cold traps at various time intervals. From the average of the last three flow rates after steady state had been reached, the flux for every experimental condition was calculated. The experimental error when measuring the flux of pure components was less than 2%.

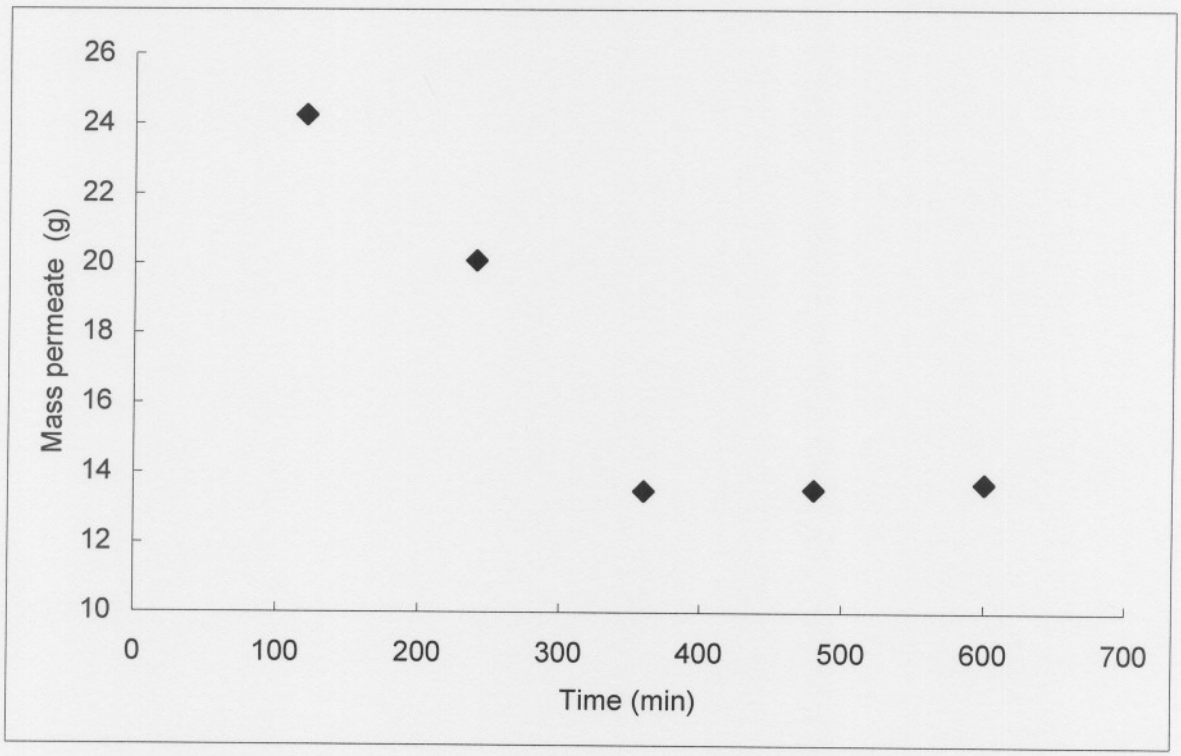


**Figure 4.5 Graph of the mass permeate as a function of time**

The influence of the feed temperature on the pervaporation flux for the single components (water and ethanol) was investigated by measuring the total flux

through the membrane as a function of the feed temperature as shown in Figure 4.6.

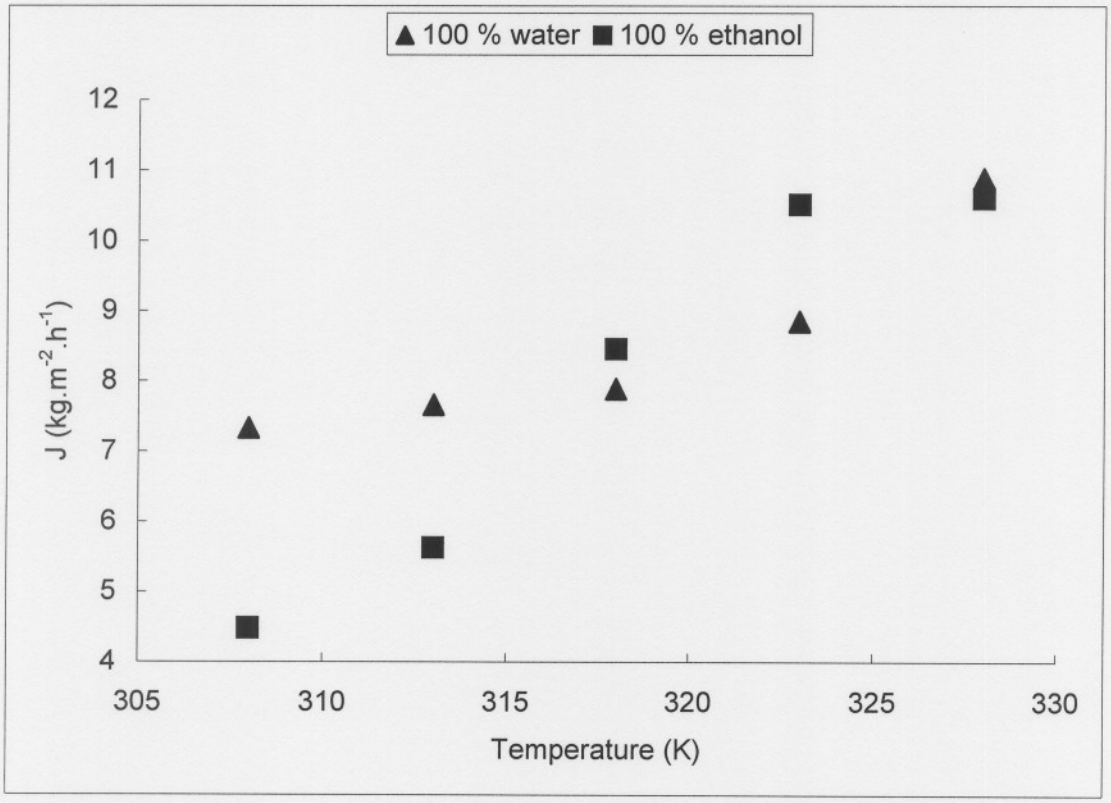


**Figure 4.6 Influence of feed temperature on pure component fluxes**

According to Figure 4.6, an increase in feed temperature resulted in an increase in flux for both ethanol and water. The increase in flux with temperature can be explained by the increase in the driving force across the zeolite membrane. The saturated vapor pressure on the feed side increases with an increase in feed temperature, while the permeate vacuum pressure remains constant. The pressure difference across the membrane thus increases with temperature and an increase in flux is observed [14, 15]. The reason for the higher water flux is related to the separation mechanism of the zeolite membrane which is based on the preferential adsorption, and the differences in the mobility of the components in the feed solution due to size and shape selectivities. The kinetic diameters of water

and ethanol are 0.31 and 0.45 nm respectively. Therefore, the permeate of the organic (ethanol) solvent is lower due to the larger molecular diameter, resulting in a decreased mobility of the ethanol. In addition, water preferentially adsorbs on the highly hydrophilic NaA-surface, increasing the preferential permeation of the water even further [7,16,17].

According to Feng and Huang [14] the apparent activation energy of the separation process can be calculated in terms of the Arrhenius type exponential relation between permeation flux and temperature using equation (4.2) [12],

$$\ln J = \ln J_0 - \frac{Ep}{RT} \qquad (4.2)$$

where J is the permeate flux ($mol.m^{-2}.h^{-1}$), $J_o$ is the pre-exponential factor, $E_p$ ($kJ.mol^{-1}$) is the apparent activation energy for permeation, R ($kJ.mol^{-1}.K^{-1}$) is the gas constant and T(K) is the absolute temperature.

The activation energy of the process can therefore be obtained by plotting the ℓn J of the permeation flux against the inverse of the temperature as shown in Figure 4.7. A straight line was fitted through the data to calculate the activation energy of pervaporation, which was found to be 39.6 $kJ.mol^{-1}$ for ethanol and 16.0 kJ $mol^{-1}$ for water, respectively. The accuracy of the fit is given by the $R^2$ which was calculated using equation (4.3),

$$R^2 = 1 - \frac{\text{Sum of squares of differences}}{\text{Sum of square}} = 1 - \frac{\sum (x-y)^2}{\sum x^2 + y^2} \qquad (4.3)$$

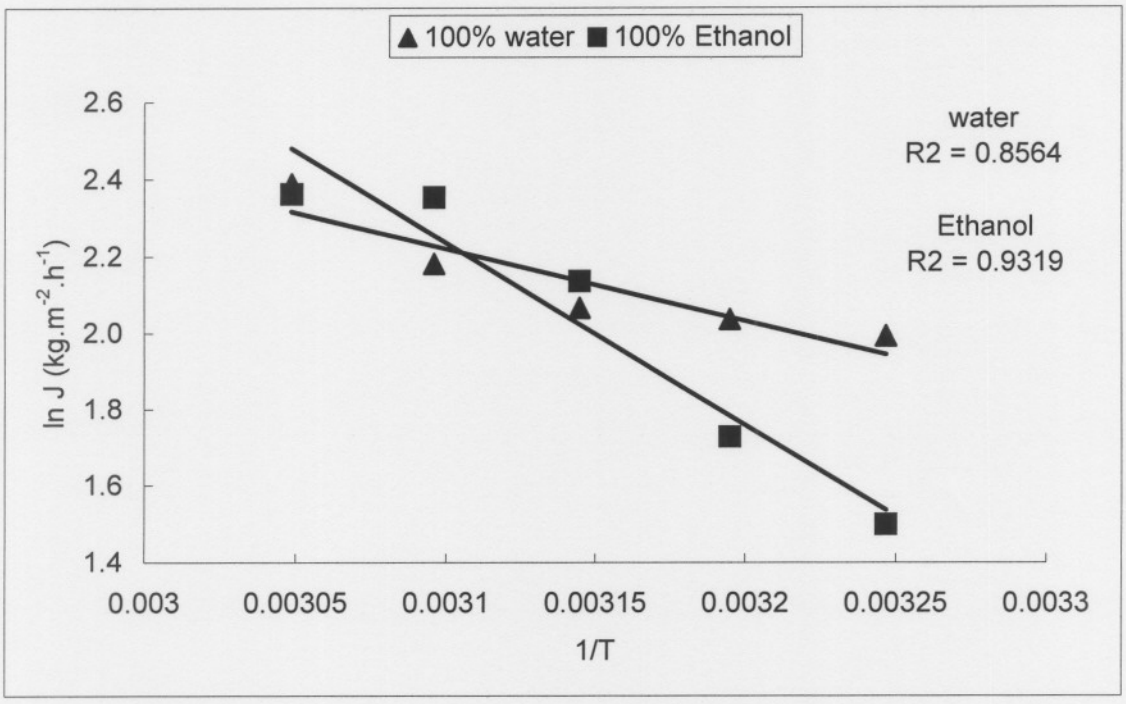


**Figure 4.7 Arrhenius plot for pure component fluxes**

The activation energy for pervaporation depends on the membrane and membrane material being used since the activation energy for pervaporation is the sum of the activation energy of diffusion and the heat of adsorption [13]. Since the activation energy of water is 23 kJ.mol$^{-1}$ lower than that of ethanol, it suggests that water requires less activation energy for diffusion, i.e. diffuses more readily than ethanol. Both Okamoto et al [31] and Casado et al [15] obtained higher values for the activation energy of the water permeation through a NaA-zeolite membrane (35 kJ.mol$^{-1}$ and 46 kJ.mol$^{-1}$, respectively) which could be contributed to the larger pore diameter of mordenite, which they used as the support for their NaA-zeolite membrane. This shows that the support also influences the activation energy of pervaporation.

In addition, temperature changes lead to changes in the pervaporation process, which could be related to changes in the kinetically controlled pervaporation process. At low temperatures, the activation energy is high since the mobility of

the molecules is low. At higher temperatures the activation energy will decrease because the mobility of the molecules increase [17].

### 4.3.2. Binary mixtures

#### 4.3.2.1. Influence of feed composition

The influence of the feed composition was determined by varying the water content in the feed from 5 to 95%. The experimental error within the single run was less than 3%, while the error between runs under identical conditions was below 10%. In Figure 4.8, the influence of the water content on the total flux is shown for two temperatures, i.e. 308K and 323K.

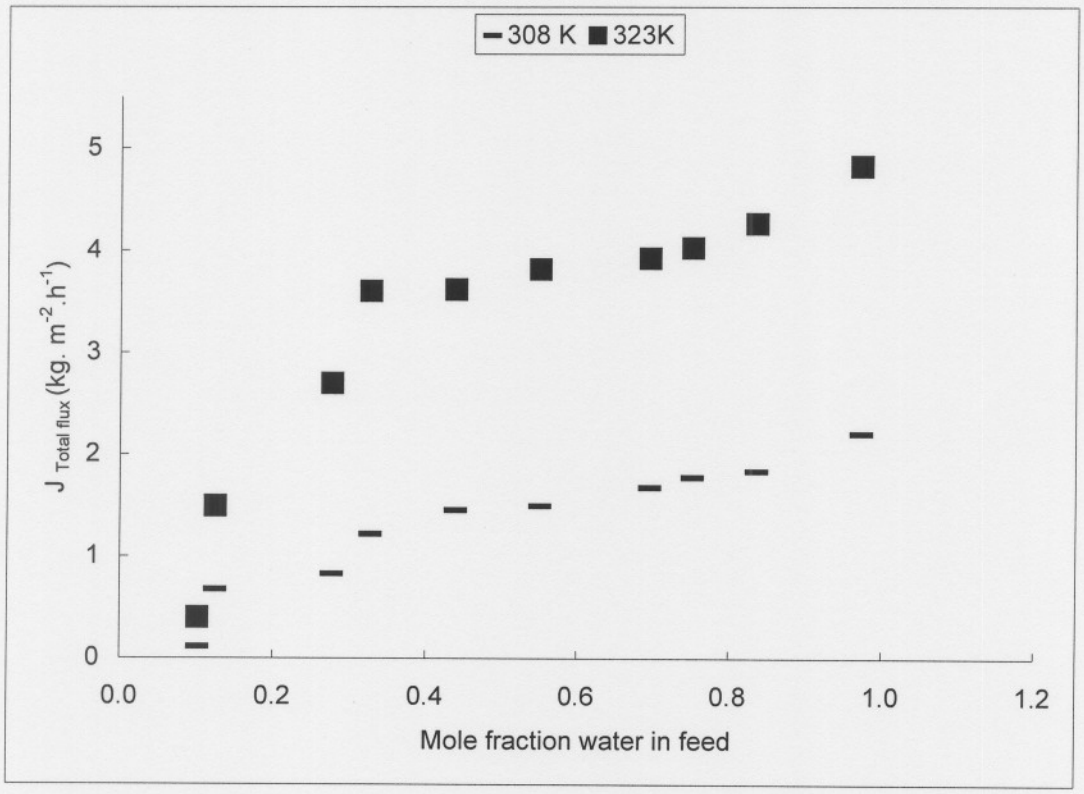


**Figure 4.8 Influence of the water content on the total pervaporation flux at 308 K and 323 K**

The total flux increases with an increase in the water concentration in the feed, a phenomenon which has previously been reported by Shah et al [4]. This increase in water flux is due to the high affinity of the NaA-zeolite for water due to its hydrophilic nature. Since the active layer of the membrane preferentially absorbs water, the water flux through the membrane remains high over a wide range of ethanol concentrations [4]. This is confirmed in Figure 4.9 where the flux of only the water fraction is presented as a function of the mole fraction of water in the feed.

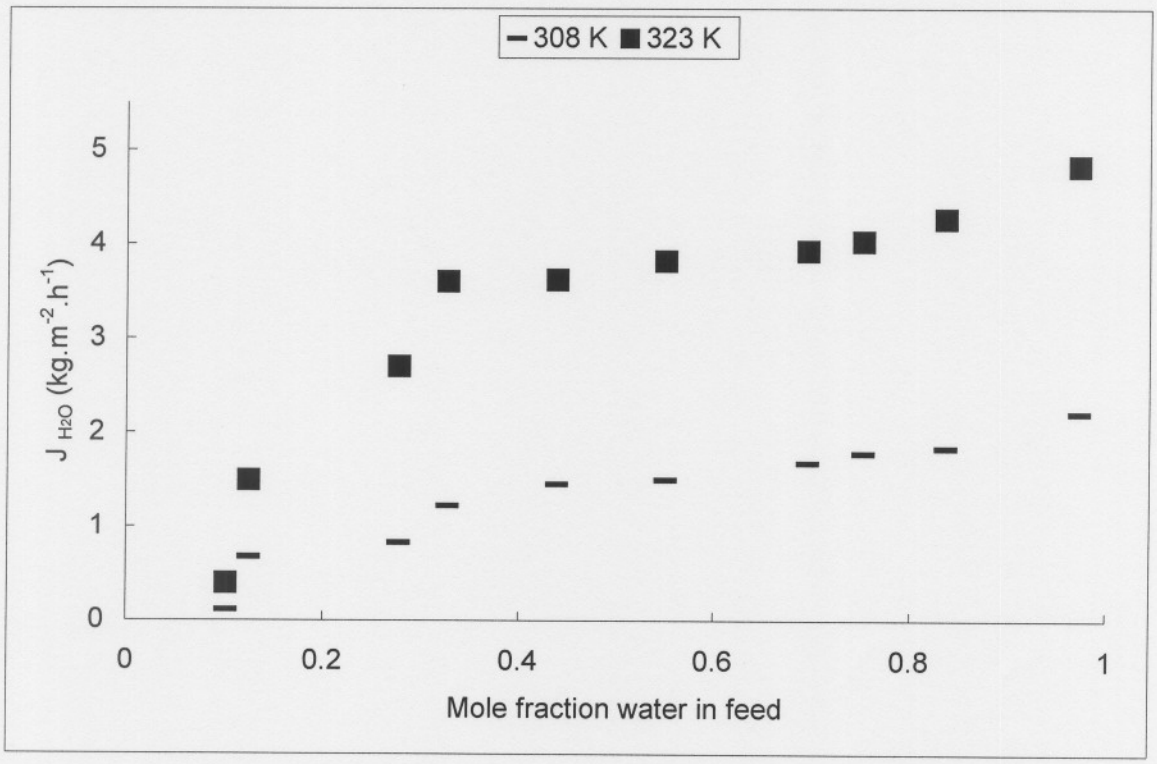


**Figure 4.9 Influence of water content on the water flux**

It is clear that the water flux follows the same trend and magnitude as the total flux, showing that the increase in total flux with increasing water content is due to the high affinity of the zeolite for water. When comparing the magnitude of the fluxes presented in Figure 4.8 and Figure 4.9, it becomes clear that the total flux is similar to the water flux both in terms of shape and magnitude. This implies that the total flux is made up mainly of water ($J_{total} = J_{water}$).

Since the effect of the temperature on a binary mixture will be discussed separately (Section 4.3.2.2), it suffices to say at this point that a definite increase in flux is observed with increasing temperature. However, the slope of the flux increase with the increase in water content seems to be independent of temperature.

The water flux increases most dramatically from 5-35% water content in the feed. Above 35% there is a slight decrease in the slope, which could result from water molecules having a higher diffusion rate through and absorption capacity on the NaA-zeolite membrane because of the smaller kinetic diameter of the water (0.31nm compared to the 0.45nm ethanol) as well as the more hydrophilic nature of the water. The water condenses within the intra- and intercrystalline pore regions of the zeolite, blocking the entry of ethanol molecules into the membrane and thus increasing the selectivity for water [7, 23, 26]. It seems that above 35% the water has condensed in all the pores of the zeolite and any further increase in the water content will thus only result in a small increase in the water flux.

While the water flux increases with an increase in the water concentration in the feed, the ethanol flux decreases (Figure 4.10), which correlates with the increase in the water flux with increasing water concentration observed in Figure 4.9. This decrease is again directly related to the condensation of water in the intercrystalline pores, which increases with the increasing water content. This means that at a low water content, numerous zeolite pores exist that are not blocked by condensed water, thus allowing the free permeation of the ethanol molecules. As the zeolite pores fill up with water with increasing water content, the ethanol flux decreases correspondingly.

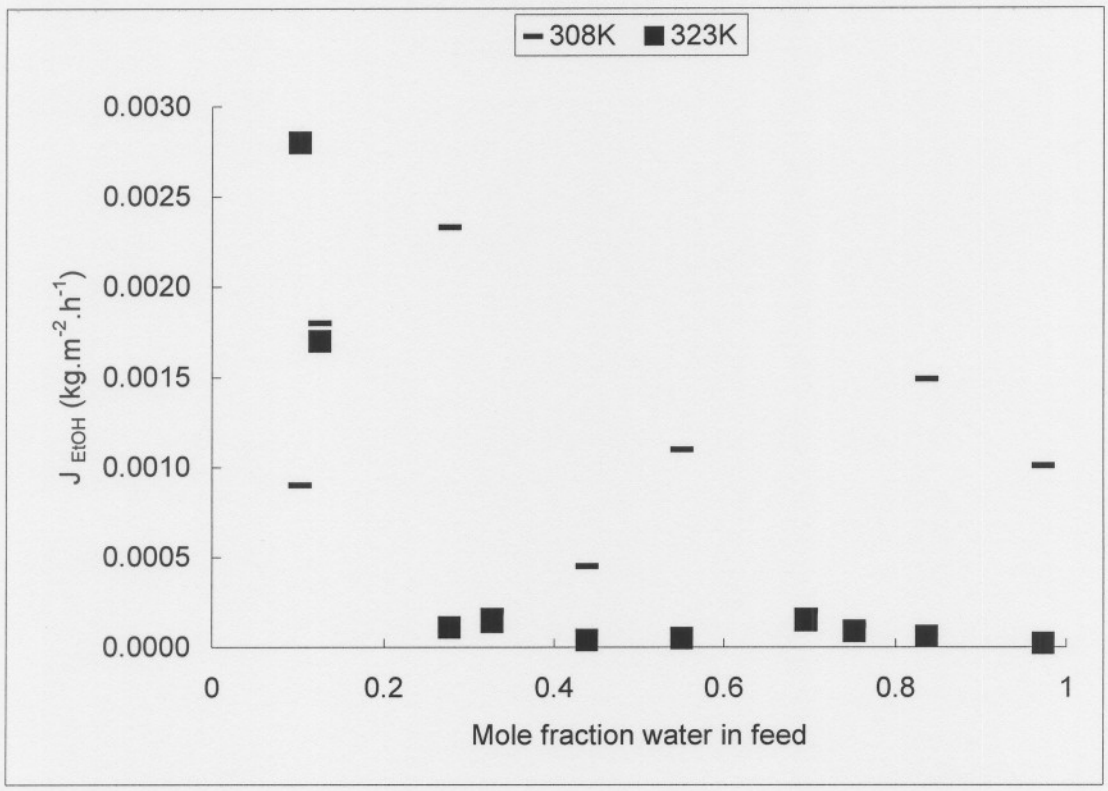


**Figure 4.10 Influence of water content on the ethanol flux**

The high ethanol flux at a low water content could also mean that, at the azeotrope (5% water), the vapor-liquid equilibrium influences the amount of each component being absorbed, due to the difference between the vapor phase composition and the liquid phase composition. Therefore, an increase in the water feed concentration beyond the azeotrope results in a decrease in the ethanol flux. This phenomenon has been previously presented by Marx [24].

It is interesting to note that, while the water flux was higher at a higher temperature, the ethanol flux decreases with increasing temperature. This decrease in the ethanol flux with increasing temperature is probably related to the decrease in the adsorption of the ethanol at elevated temperatures due to the increase in energy in the system. This effect can clearly be seen when plotting the

separation factor of water and ethanol as a function of the mole fraction water in the feed (Figure 4.11).

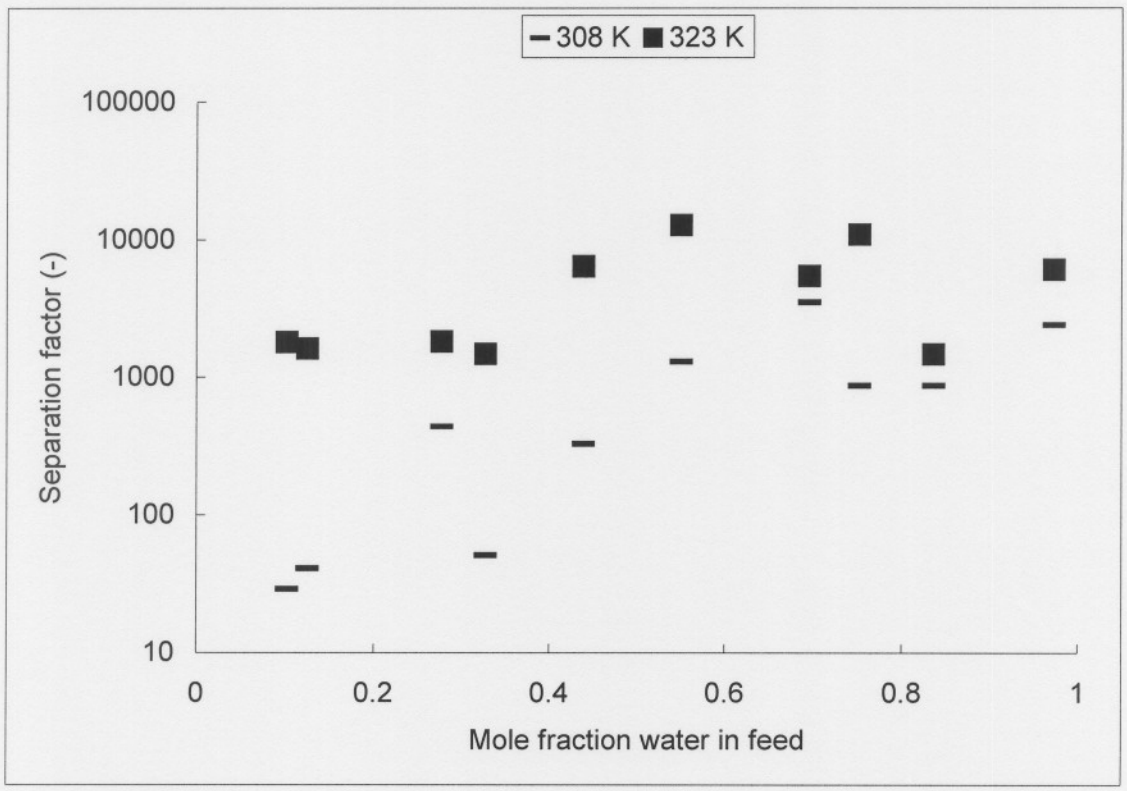


**Figure 4.11 Influence of feed composition on the selectivity of the membrane**

It can be seen that there was an increase in selectivity at the lower temperature (308 K) until the water content reached 50 %. Increasing the water content above 50 % had no further significant influence on the selectivity in spite of the increase in total flux. It is possible that the initial increase in selectivity with increasing water content is the result of the increased condensation in the intercrystalline pores, restricting the ethanol permeation while facilitating the water permeation [25]. The constant selectivity at higher water content could indicate that all the intercrystalline pores have been filled with water, which implies that a higher water content would not contribute to an increase in selectivity. The increase in selectivity with the

increased temperature is the direct result of the inverse effect the temperature had on the water flux compared to the ethanol flux. [26]

#### 4.3.2.2. Influence of feed temperature

The influence of the feed temperature on the total, water and ethanol pervaporation flux is shown in Figure 4.12, Figure 4.13 and Figure 4.14, respectively. According to Figure 4.12 and Figure 4.13, the total and water flux increase linearly with an increase in temperature as had been obtained for the pure components (see Figure 4.6). This could either be the result of an increase in mobility of the mixture molecules when the temperature is raised and the diffusion of water in the membrane increases, or an increase in adsorption [7, 26].

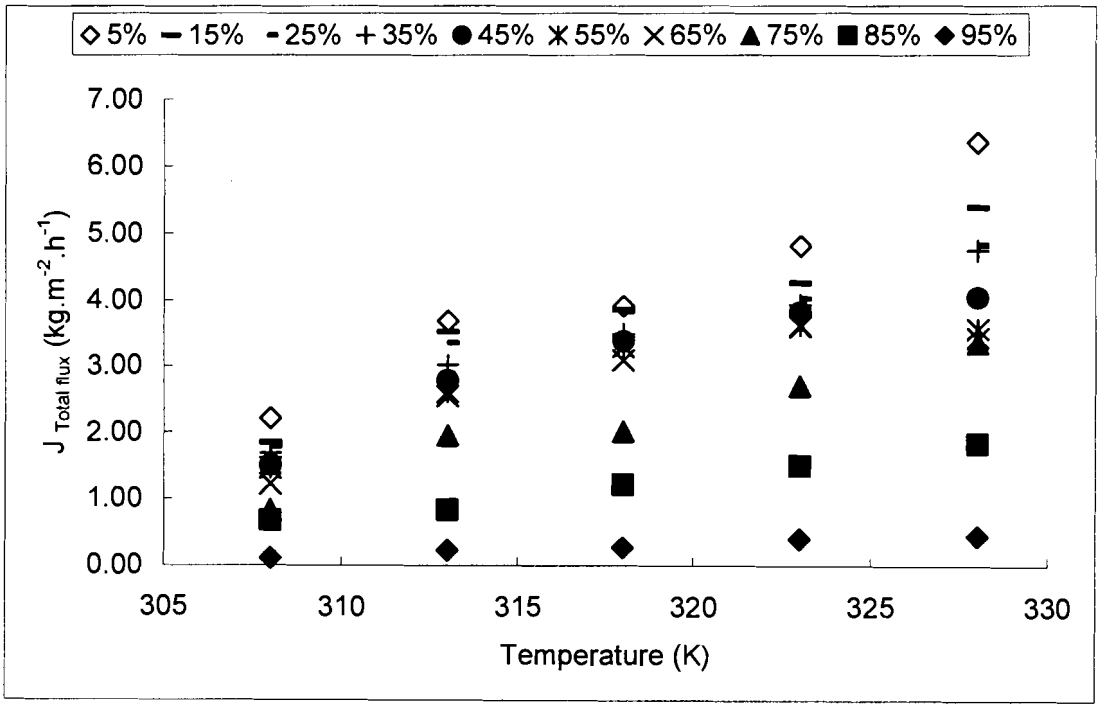


**Figure 4.12 Influence of temperature on the total pervaporation flux (legend = mole % of water)**

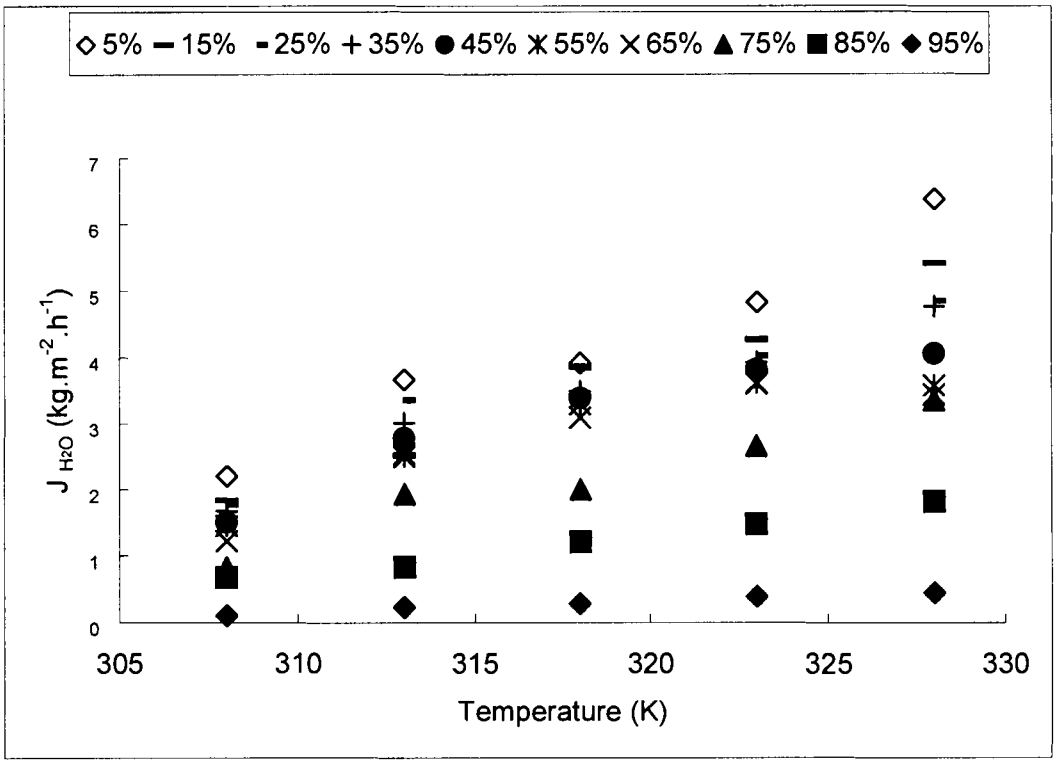


**Figure 4.13 Influence of temperature on the water flux (legend = mole % of water)**

While the flux of ethanol as a single component increased with increasing temperature (Figure 4.6), in mixtures the amount of ethanol permeating remains practically constant with a increase in temperature (Figure 4.14). This again shows that diffusion in mixtures can be significantly different from pure component diffusion because molecules influence the diffusion of other molecules, and thus exhibit correlation effects [27]. When comparing the flux of ethanol as a single component (Figure 4.6) to the flux in a binary mixture, a 1000 fold decrease is observed. This can be explained by the condensation of water in the intercrystalline pores inhibiting the permeation of ethanol. When there is no water present, the ethanol can freely permeate through all the pores, explaining why similar fluxes where observed for water and ethanol when working with single components. As expected, the highest ethanol flux was obtained when the least water was present (see also Figure 4.10).

According to Bowen et al [28], molecular simulation of multicomponent diffusion through zeolite pores indicate that slower molecules sometimes inhibit diffusion of faster molecules because molecules have difficulty passing one another in the zeolite pores. This is in agreement with this study where the water as a single component reaches flux above 10 $kg.m^{-2}.h^{-1}$ at 328 K (Figure 4.6), compared to the water flux of above 6 $kg.m^{-2}.h^{-1}$ in the presence of 5% ethanol at 328 K.

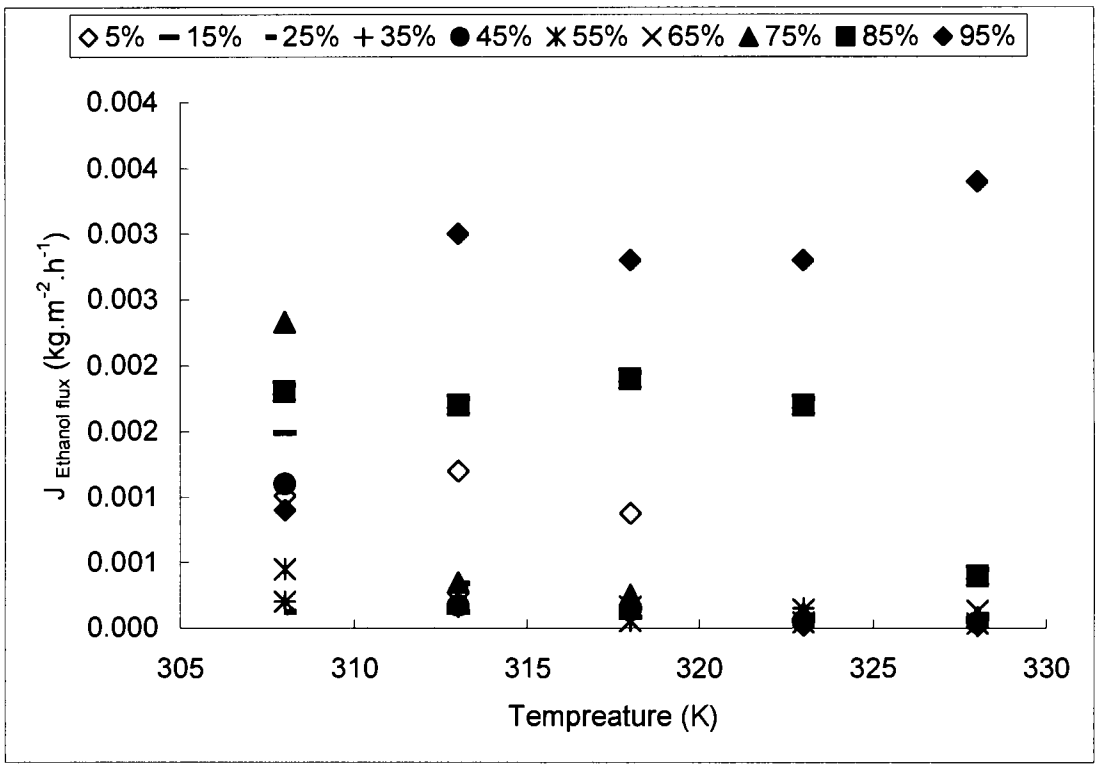


**Figure 4.14 Influence of temperature on the ethanol flux (legend = mole % of water)**

The influence of temperature on the selectivity is shown in Figure 4.15. In general, there was an increase in selectivity with an increase in temperature. This could mean that the adsorption of alcohol is inhibited by the presence of water, as this adsorbs strongly in the zeolite and non-zeolite pores of the NaA-zeolite membrane and blocks the organic (ethanol) molecules from entering the pores. It could also

imply that the increase in temperature has a strong effect on the adsorption of the ethanol onto the zeolite, which would result in an increase in selectivity. Judging from the high selectivity of 19832, it is reasonable to suggest that the NaA-zeolite membrane does not have substantially larger penetrating non-zeolite pores which would have caused a decrease in selectivity [7]. For all practical purposes, the zeolite membrane can thus be regarded as defect free.

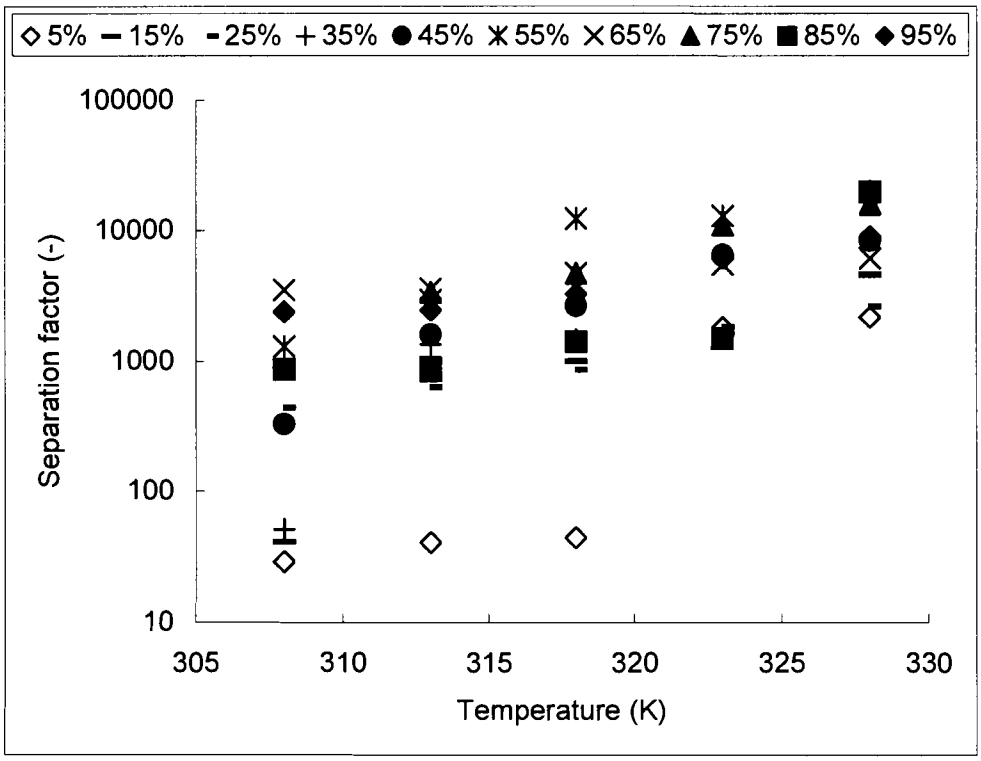


**Figure 4.15 Influence of temperature on the selectivity of the membrane (legend = mole % of water)**

### 4.3.3. Effect of membrane thickness

While the previous section has dealt purely with a single coated NaA-membrane, in Table 4.1 and 4.2 the influence of membrane thickness on flux and selectivity for both single and double coated NaA membranes varying the feed temperature and the composition is presented. Both flux and selectivity decreased when the

thickness of the membrane increased from 5 to 10μm, which has not been expected in terms of the selectivity since usually, according to literature, the selectivity increases with an increase in membrane thickness while the flux decreases [29, 30]. Judging from the average selectivity of only 4308 for the double coated membrane it seems that the double-coated membrane must have had defects, which caused the decrease in selectivity

**Table 4.1: Total flux and separation factor (α) of a single coated NaA-zeolite membrane**

| Temperature (K) | Feed (EtOH wt %) | Total flux ($kg.m^{-2}.h^{-1}$) | Separation factor (α) |
|---|---|---|---|
| 308 | 95 | 0.11 | 2396 |
| | 55 | 1.46 | 1297 |
| | 15 | 1.84 | 41 |
| 323 | 95 | 0.45 | 8851 |
| | 15 | 5.40 | 4597 |

**Table 4.2: Total flux and separation factor (α) of double coated NaA-zeolite membrane**

| Temperature (K) | Feed (EtOH wt %) | Total flux ($kg.m^{-2}.h^{-1}$) | Separation factor (α) |
|---|---|---|---|
| 308 | 95 | 0.38 | 3073 |
| | 55 | 0.55 | 203 |
| | 15 | 0.72 | 29 |
| 323 | 95 | 0.70 | 4308 |
| | 15 | 1.18 | 247 |

## 4.4. Comparison of pervaporation data

In Table 4.3, the results of the separation of an ethanol/water mixture by pervaporation using zeolite NaA-membranes coated on different supports from different literature studies were compared. According to this table, little correlation exists between the performance of the membrane (flux and selectivity) on the one hand, and temperature and membrane thickness on the other hand. Contrary to expectations, one of the best results for both flux and selectivity had been obtained with a very thick zeolite layer [10]. Similarly, the flux and selectivity seemed to be independent of temperatures used, ranging from 50 $^0$C [6] to 125 $^0$C [9]. From all these results, it is clear that the most important variable determining efficiency of a membrane is the manufacturing of the membrane, including the type and smoothness of the support that has been used. This could imply that the optimised conditions for pervaporation might differ depending on the support and method of zeolite synthesis.

**Table 4.3: Results of studies on the separation of ethanol/water mixtures by pervaporation using zeolite NaA-membranes**

| Support | Membrane Thickness (μm) | Water content (wt %) | Temperature (°C) | Flux ($kg.m^{-2}.h^{-1}$) | Selectivity | Reference |
|---|---|---|---|---|---|---|
| Ceramic | - | 10 | 60 | 2-0.05 | 5000 | [4] |
| Ceramic | - | 10 | 60 | 1.5 | 16000 | [5] |
| Ceramic | 10 | 10 | 50 | 0.772 | 46000 | [6] |
| Ceramic | 10 | 5 | 50 | 0.396 | 48000 | |
| Ceramic | 10 | 1.0 | 50 | 0.079 | 500 | |
| Ceramic | 10 | 5 | 50 | 0.004 | 470 | |
| Ceramic | 30 | 10.3 | 75 | 2.15 | 10000 | [8] |
| Ceramic | 15 | 10 | 125 | 3.80 | 3603 | [9] |
| Ceramic | 20-30 | 10 | 105 | 4.53 | 30000 | [10] |
| Ceramic | 10 | 5 | 75 | 1.10 | 10000 | |
| Ceramic | 5 | 5 | 55 | 4.50 | 19832 | This work |
| Ceramic | 10 | 5 | 55 | 0.70 | 4308 | This work |
| Mullite | 10 | 5 | 75 | 2.08 | 42000 | [6] |
| γ-alumina | 10-30 | 5 | 70 | 0.0006 | 18000 | [7] |
| Ceramesh | 10 | 10 | 70 | 1.0 | 100000 | [11] |
| Carbosep | 10 | 10 | 70 | 0.3 | 10000 | |

## 4.5. Conclusion

NaA-zeolite coated tubular ceramic membranes manufactured in-house were investigated to determine their pervaporation characteristics. It was found that pervaporation could be used to separate azeotropic mixtures like the water/ethanol mixture used in this study. Since the NaA-zeolite membrane is hydrophilic, water permeates preferentially. Selectivities as high as 20000 with a flux of 4.5 $kg.m^{-2}.h^{-1}$ have been obtained. This confirms that a defect free NaA-membrane has been manufactured for the single coated membrane.

It was further shown that both the water flux and the total flux increased with an increasing water content in the mixture, while the ethanol flux decreased with an increasing water content.

Water was found to be preferentially absorbed in the membrane and the increase in temperature had a significant influence on the transport of the molecules through the membrane. By increasing the temperature the mobility of the molecules is increased resulting in an increase in total flux.

In this study it was found that the thinner (5 μm) membrane produced higher selectivities than the thicker (10 μm) membrane, i.e. the selectivity decreased with an increase in membrane thickness which was ascribed to defects within the double coated membrane.

## 4.6. References


[1] G.C. Steenkamp, K. Keizer, H.W.J.P. Neomagus and H.M. Krieg, 2002, Copper (II) removal from polluted water with alumina/chitosan composite membranes, Journal of Membrane Science, **197**, 147-156

[2] M.M.J. Treacy, J. B. Higgins, 2001, Collection of simulated XRD powder patterns for zeolites, 4th Edition Elsevier Amsterdam,

[3] Y. K. Hong and W.H. Hong, 1999, Influence of ceramic support on pervaporation characteristics of IPA/water mixtures using PDMS/ceramic membrane, Journal of Membrane Science, **159**, 29-39

[4] D. Shah, K. Kissick, A. Ghorpade, R. Hannah and S. Bhattacharyya, 2003, Pervaporation of alcohol-water and dimethylformamide–water mixtures using hydrophilic zeolite NaA membranes: mechanisms and experimental results, Journal of Membrane Science, **215** 235-247

[5] T. Gallego-Lizon, E. Edwards, G. Lobiundo and L. Santos, 2002, Dehydration of water/t-butanol mixtures by pervaporation: Comparative study of commercially available polymeric microporous silica and zeolite membranes, Journal of Membrane Science, **197**, 309-319

[6] M. Kondo, M. Komori, H. Kita and K. Okamoto, 1997, Tubular-type pervaporation module with zeolite NaA membrane, Journal of Membrane Science, **133**, 133-141

[7] S. Sommer and T. Melin, 2005, Performance evaluation of microporous inorganic membranes in the dehydration of industrial solvents, Chemical Engineering and Processing, **44**, 1138-1156

[8] H. Kita, K. Horri, Y. Ohtoshi, K.Tanaka and K. Okamoto. 1995, Synthesis of a zeolite NaA membrane for pervaporation of water/organic liquid mixtures, Journal of Material Science Letters, **14**, 206-208

[9] M. P. Pina, M. Arruebo, M. Felipe, F. Fleta, M.P. Bernal, J. Coronas, M. Menéndez and J. Santamaria, 2004, A semi continuous method for the synthesis of NaA zeolite membranes on tubular support, Journal of Membrane Science, **244**,141-150

[10] Y. Morigami, M. Kondo, J. Abe, H. Kita and K. Okamoto, 2001, The first large scale pervaporation plant using tubular-type module with zeolite NaA

[11] J.J. Jafar and P.M. Budd, 1997, Separation of alcohol/water mixture by pervaporation through zeolite A membrane, Microporous Materials, **12**, 305-311

[12] X. Feng, Estimation of activation energy, 1996, Journal of Membrane Science **118**, 127-131

[13] A.A. Kittur, S.S. Kulkarni, M.I. Aralaguppi and M.Y. Kariduraganavar, 2005, Preparation and characterization of novel pervaporation membranes for the separation of water–isopropanol mixtures using chitosan and NaY zeolite, Journal of Membrane Science, **247**, 75-86

[14] X. Feng and R.Y.M. Huang, 1996, Pervaporation with chitosan membranes: I Separation of water from ethylene glycol by a chitosan/polysulfone composite membrane, Journal of Membrane Science, **116**, 67

[15] L. Casado, R. Mallada, C. Téllez, J. Coronas, M. Menéndez and J. Santamaria, 2003, Preparation, characterisation and pervaporation performance of mordent membranes, Journal of Membrane Science, **216**, 135-147

[16] R. M. de Vos and H. Verweij, 1998, Improved performance of silica membranes for gas separation, Journal of Membrane Science, **143**, 37-51

[17] B. Adnadjevic, J. Jovanovic and S. Gajinov, 1997, Effect of different physicochemical properties of hydrophobic zeolites on the pervaporation properties of PDMS-membranes, Journal of Membrane Science, **136**, 173-179

[18] T. Mohammadi, A. Aroujalian and A. Bakhshi, 2005, Pervaporation of dilute alcoholic mixtures using PDMS membranes, Chemical Engineering Science, **60**, 1875-1880

[19] G. Qunhui, H. Ohya and Y. Negishi, 1995, Investigation of the permselectivity of chitosan membrane used in pervaporation separation: II

Influence of temperature and membrane thickness, Journal of Membrane Science, **98**, 223-232

[21] R.Y.M. Huang and C.K. Yeom, 1991, Pervaporation separation of aqueous mixtures using crosslinked poly (vinyl alcohol). II Permeation of ethanol-water mixtures, Journal of Membrane Science, **53**, 33

[22] Y.M. Lee, E.M. Shin and S.T. Noh, 1991, Pervaporation separation of water-ethanol through modified chitosan membranes. 3. Sulfonated chitosan membranes, Polymer **15**, 497

[23] J.C. Jansen, J.H. Koegler, H. van Bekkum, H.P.A. Calis, C.M. van den Bleek, F. Kapteijn, E.R. Geus and N. van der Puil, 1998, Zeolite coatings and their potential use in catalysis, Microporous and Mesoporous Materials, **21**, 213-226

[24] S. Marx, 2002, Potchefstroom University for Christian Higher Education, Application of pervaporation to the separation of methanol from tertiary amyl methyl ether, Thesis, 63

[25] S. Sommer and T. Melin, 2005, Influence of operation parameter on the separation of mixture by pervaporation and vapor permeation with inorganic membranes. Part I: Dehydration of solvents, Chemical Engineering Science, **60**, 4509-4523

[26] G. Li, E. Kikushi and M. Matsukata, 2003, A study on the pervaporation of water-acetic mixtures through ZSM-5 zeolite membrane, Journal of Membrane Science, **218**, 185-194

[27] G.S. Luo, M. Niang and P. Schaetzel, 1997, Pervaporation separation of ethyl tert-butyl ether and ethanol mixtures with a blended membrane, Journal of Membrane Science, **125**, 237-244

[28] T.C. Bowen, J.C. Wyss, R.D. Noble and J. L. Falconer, 2004, Measurement of diffusion through a zeolite membrane using isotopic-transient pervaporation, Microporous and Mesoporous Materials, **71**, 199-210

[29] P. Kanti, K. Srigown, J. Madhur, B. Smitha and Sridhar, 2004, Dehydration of ethanol through blend membranes, of chitosan and sodium alginate by pervaporation, Separation and Purification Technology, **40**, 259-266

[30] J.P.G. Villaluenga, M. Khayet, P. Godino, B Seoane and J. B. Mengual, 2003, Analysis of the membrane thickness effect on the pervaporation of methanol/methyl tertiary butyl ether mixtures, Separation and Purification Technology, **47**, 80-87

[31] K. Okamoto, H. Kita, K. Korrii, and K. Tanaka, 2001, Zeolite NaA membrane: preparation single-gas permeation and pervaporation and vapor permeation of water/ organic liquid mixtures, Ind. Eng. Chem. Res, 40, 163

# Chapter 5

# EVALUATION

## 5.1. Ceramic support

The inner surface of the tube of a ceramic support prepared by centrifugal casting is shown in Figure 5.1 (a), while the surface of a support prepared by extrusion is shown in Figure 5.1 (b). With centrifugal casting, the packing is regular and the surface is smooth, which makes supports prepared by this method ideal for the direct coating with thin, defect free zeolite layers.

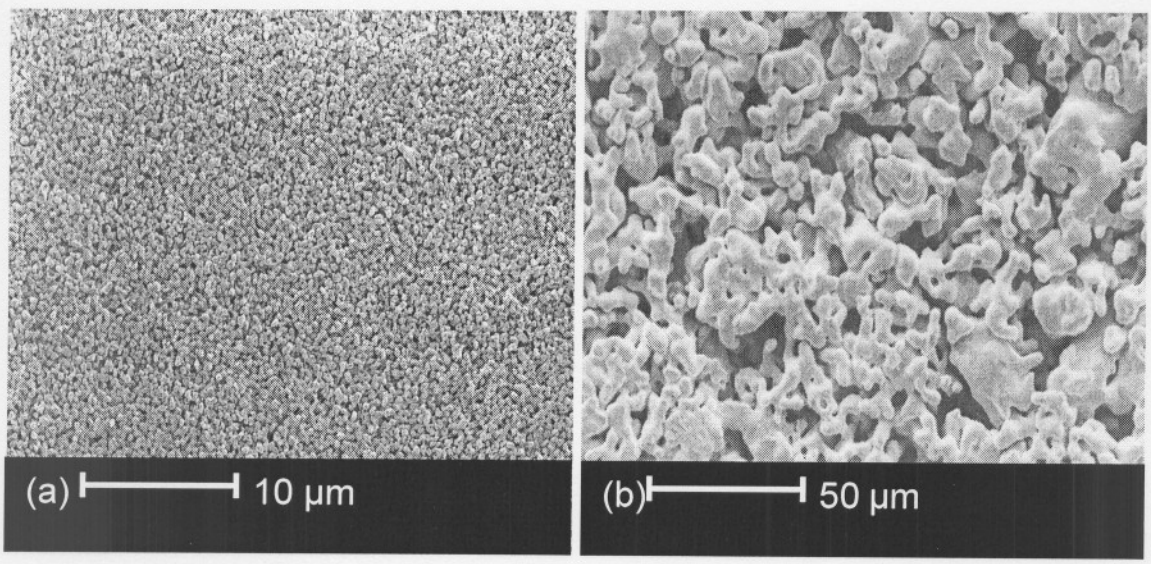


**Figure 5.1** **SEM-micrograph of the inner surface of a (a) centrifugally casted and (b) intrusion or mold casted ceramic support**

Since the support made by extrusion or mold casting (Figure 5.1 (b)) has both defects and an irregular packing, a thicker zeolite layer would be required (in theory) to ensure a defect free coating.

## 5.2. Zeolite NaA-coating

Figure 5.2 shows a SEM-micrograph that reveals a cross-section of (a) a single layer and (b) a double layer of NaA coated onto the ceramic support. Complete coverage was obtained after only one coating with an average membrane thickness of 5 µm (Figure 5.2 (a)). Due to the use of a centrifugally casted support, it was then possible to coat the ceramic with a thin, as well as defect free, zeolite NaA-layer without requiring the use of an additional layer as is commonly the case for extruded ceramic supports.

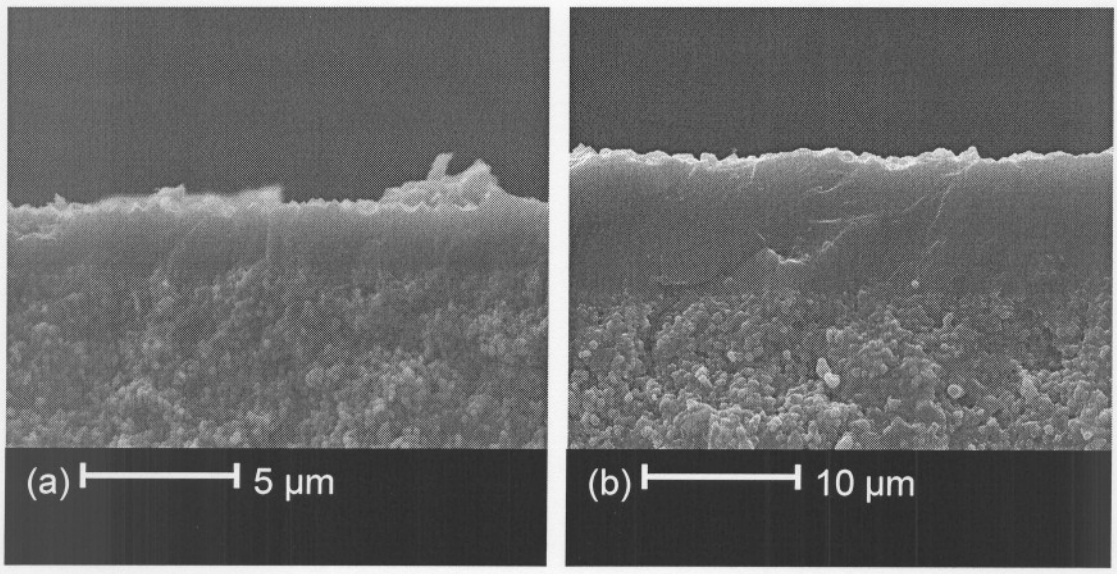


**Figure 5.2** **SEM-micrograph (cross-section) of a densely intergrown cubic zeolite NaA-crystal layer grown on an AKP-15 support surface for single coating**

According to Figure 5.2 (b), the second layer was again completely intergrown with the first layer. The total thickness of a double coated zeolite NaA-layer was 10 µm on average. The synthesis period for this membrane was 4 hours.

The correct zeolite type (NaA) was confirmed both by SEM (cubic structure) and by XRD, where the surface diffractogram of all growth layers correlated with the simulated framework diffractogram for hydrated zeolite LTA. According to XRD, the manufactured zeolite consisted solely of NaA with no other crystalline impurities present.

The graph presented in Figure 5.3 summarises the fluxes and selectivities obtained for the pervaporation of a binary water/ethanol mixture through a single coated NaA-composite membrane. Each data point is a series of a specific mole fraction of water which was obtained at a specific temperature. For example, at 5% water there was a sharp increase in selectivity and a slight increase in flux with increasing temperature.

In general there was an increase both in the selectivity and water flux with an increase in the water content in the feed. The optimal flux as a function of the separation factor was observed when the water content was between 55 and 75% in the feed, which distinctly showed the influence of the feed composition on both flux and selectivity. It can clearly be seen that, at high ethanol concentrations, both selectivity and flux are very low, which confirms that the NaA-zeolite membrane used in this study has a high affinity for water. The highest fluxes were obtained at 95% water, which was, however, at the cost of the selectivity.

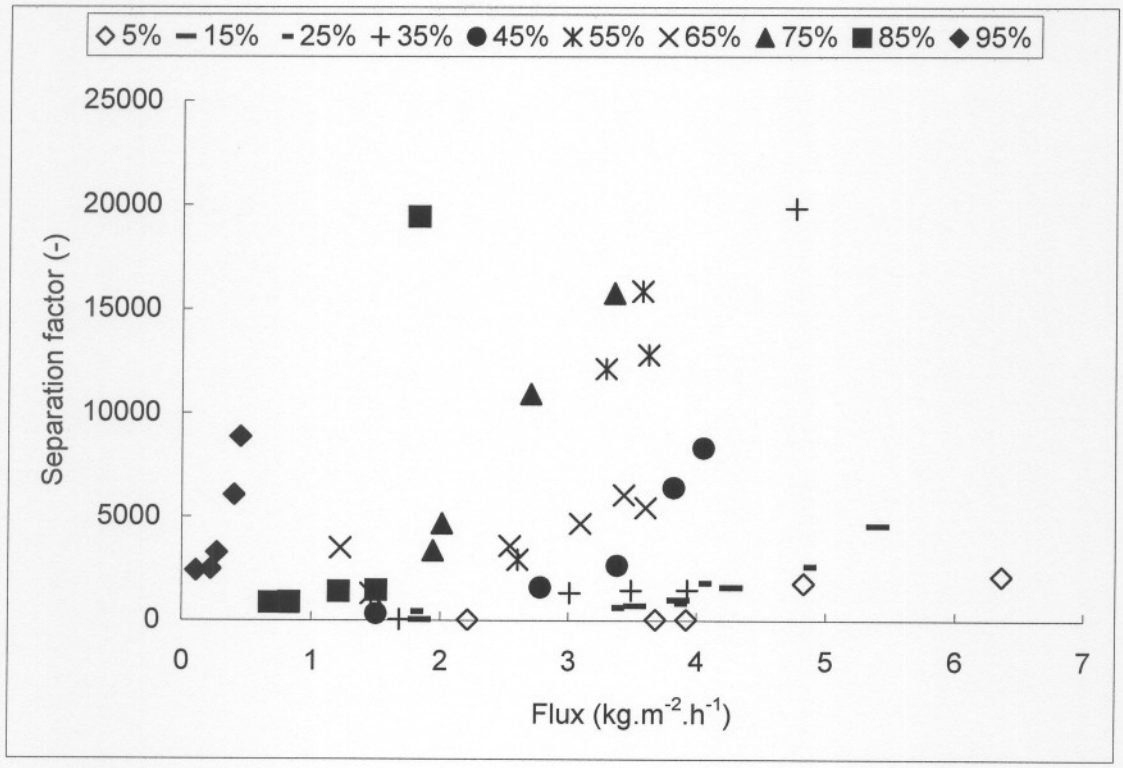


**Figure 5.3** **Separation factor presented as a function of flux (legend = mole % of water)**

When comparing the best pervaporation results obtained in this study for the single and double layer coated composite membranes with studies presented in literature, the following graph is obtained (Figure 5.4). According to Figure 5.4, where the separation factor is presented as a function of flux, it is especially the single coated membrane that compares favourably with literature. Although much higher selectivities had been obtained according to literature, the in-house manufactured single coated membrane had an above average flux as well as an above average selectivity.

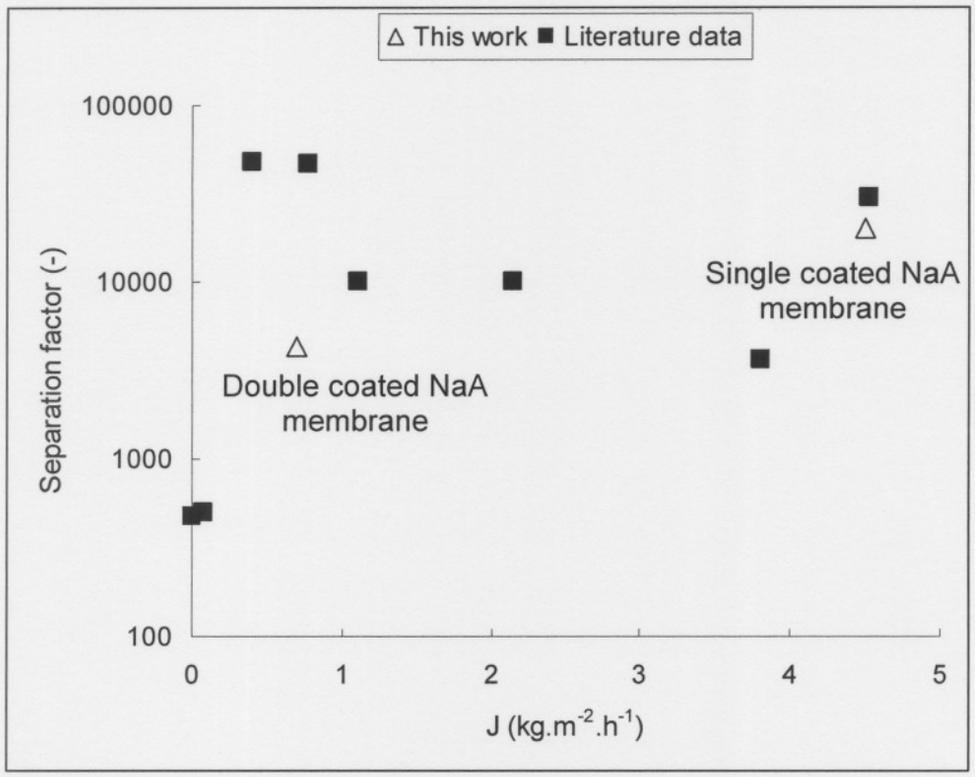


**Figure 5.4 Comparing flux against selectivity as reported in literature with results from this work**

## 5.3. Conclusion

Defect free single and double coated NaA-ceramic composite membranes have been successfully manufactured by the direct coating of the zeolite on the smooth inside surface of a centrifugally casted tubular ceramic membrane.

During the characterization of the composite membrane, using the pervaporation of water and ethanol mixtures at different temperatures and molar ratios, it was shown that especially the single coated membrane yielded a very high flux at above average selectivities. It was further shown that both the flux and the separation factor increased with increasing temperature.

## 5.4. Recommendation

Future experimental work that can be recommended for investigation, which was not covered by this study, includes a comparison between liquid permeation and vapor permeation. This could help explain pervaporation data while determining if pervaporation as a process is equivalent to either liquid permeation or vapor permeation. It is also recommended that the double coated NaA-zeolite membrane should be further improved because of the comparatively low selectivities obtained.

More detailed research is needed to determine how the feed flow rate influences the pervaporation performance characteristics. This could be done by fixing the experimental conditions and then varying the feed flow rate over a wider range.

# GAS CHROMATOGRAPHY

# APPENDIX A

The composition of the ethanol-water mixtures were analysed using a gas chromatograph (Carlo Erbo GC 6000 Vega series 2) with a flame induced detector and a capillary column (HP-FFAP). In order to obtain concentration values a calibration curve was required.

## A.1 Preparation of standard sample

10.047g of ethanol was weighed and diluted with water to a total mass of 47.85g (20 wt% ethanol), to ensure that all peaks fell within the range of the calibration assay. From the 20 wt% ethanol solution a dilution series was prepared as shown in Table A.1. This series was called the standard ethanol solution.

**Table A.1 Preparation of the diluted calibration series for ethanol**

| | **0.1 wt%** | **1.0 wt%** | **1.5 wt%** | **2.0 wt%** | **2.5 wt%** |
|---|---|---|---|---|---|
| Mass of 20wt% EtOH solution | 0.254 | 2.564 | 3.760 | 5.267 | 6.239 |
| Diluted to total mass (g) | 49.669 | 49.572 | 49.496 | 49.701 | 49.435 |

Subsequently a standard dilution of acetonitrile (ACN) was prepared by weighing 3.064g of ACN and diluting it with water to a total mass of 25.032g. This standard solution (ACN) was used to prepare the calibration samples by further diluting 0.1g of the standard ACN solution with 0.9g of the diluted

standard ethanol solution (Table A.1) to make a total of 1g, for the ranges shown in Table A.2.

**Table A.2 Preparation of the standard sample for the GC analysis**

| | **0.1 wt%** | **1.0 wt%** | **1.5 wt%** | **2 wt%** | **2.5 wt%** |
|---|---|---|---|---|---|
| Standard solution ACN (g) | 0.107 | 0.104 | 0.123 | 0.175 | 0.168 |
| Standard solution EtOH (g) | 0.93 | 0.94 | 0.90 | 0.91 | 0.90 |
| Total mass (g) | 1.037 | 1.041 | 1.008 | 1.016 | 1.008 |

## A.2 GC analysis

The five samples (0.1-2.5 wt%) were injected three times to determine and ensure the accuracy of the calibration curve as shown in Table A.3. SS1 to SS5 refers to the weight fractions of 0.1 to 2.5 wt% respectively.

**Table A.3 Calibration data obtained from the gas chromatography analysis**

| **Sample name** | **Area (EtOH)** | **Area (ACN)** | **Area (EtOH)/Area (ACN)** |
|---|---|---|---|
| **SS1** | 40516.2 | 186675.8 | 0.217 |
| | 21980.7 | 228065.3 | 0.096 |
| | 5152.34 | 91144.83 | 0.057 |
| **Average** | **22549.75** | **168628.6** | **0.12** |
| **SS2** | 64838.68 | 58337.03 | 1.111 |
| | 234794.8 | 204863.1 | 1.146 |
| | 346286.5 | 285236.9 | 1.214 |
| **Average** | **215306.7** | **182812.4** | **1.157** |

| | | | |
|---|---|---|---|
| **SS3** | 94556.98 | 64595.1 | 1.464 |
| | 406047.1 | 255616.5 | 1.588 |
| | 378349.7 | 231030.1 | 1.637 |
| **Average** | **292984.6** | **183747.2** | **1.56** |
| **SS4** | 106670.8 | 49536 | 2.15 |
| | 109622.9 | 50170.45 | 2.19 |
| | 225653 | 96816.13 | 2.33 |
| **Average** | **147315.8** | **65507.53** | **2.22** |
| **SS5** | 124004 | 48960.8 | 2.53 |
| | 162040.2 | 64971.75 | 2.49 |
| | 858514.8 | 324597.9 | 2.64 |
| **Average** | **381519.7** | **146176.8** | **2.55** |

The average area ratios ($A_{EtOH}/A_{ACN}$) obtained from the three injections (Table A.3) were used to calculate the molar ratios ($n_{EtOH}/n_{ACN}$) for the calibration curve (Table A.4) which was calculated as follows for the 0.1wt% standard solution :

Mass $_{EtOH}$ = Total mass of sample – mass of ACN

= 1.037g - 0.107g

= 0.93g

Since the molar mass of ethanol is 46g.mol$^{-1}$.

Mole $_{EtOH}$ = (10.047g / 47.85g) × (0.254g / 49.669g) × (0.93g / 46g.mol$^{-1}$)

= 2.0 × 10$^{-5}$ mol

Mass $_{ACN}$ = Total mass of sample – mass of ACN

=1.037g - 0.93g

= 0.107g

(Molar mass of ACN is 41.05g.mol$^{-1}$)

Mole$_{ACN}$ = (3.064g / 25.032g) × (0.107g / 41.05g.mol$^{-1}$)

= 3.2 × 10$^{-4}$ mol

$n_{EtOH}/n_{ACN}$ =mole (EtOH) / mole (ACN)

$=2.0 \times 10^{-5}$ mol / $3.2 \times 10^{-4}$ mol

$=6.3 \times 10^{-2}$

**Table A.4 Calibration data for the standard curve of the GC analysis**

| | Ratio | |
|---|---|---|
| Wt% Ethanol | $A_{EtOH}/A_{ACN}$ | $n_{EtOH}/n_{ACN}$ |
| 0.1 | 0.12 | 0.063 |
| 1.0 | 1.06 | 0.703 |
| 1.5 | 1.59 | 1.051 |
| 2.0 | 2.25 | 1.467 |
| 2.5 | 2.61 | 1.739 |

From the data in Table A.4, Figure A.1 was drawn and a straight-line graph was obtained.

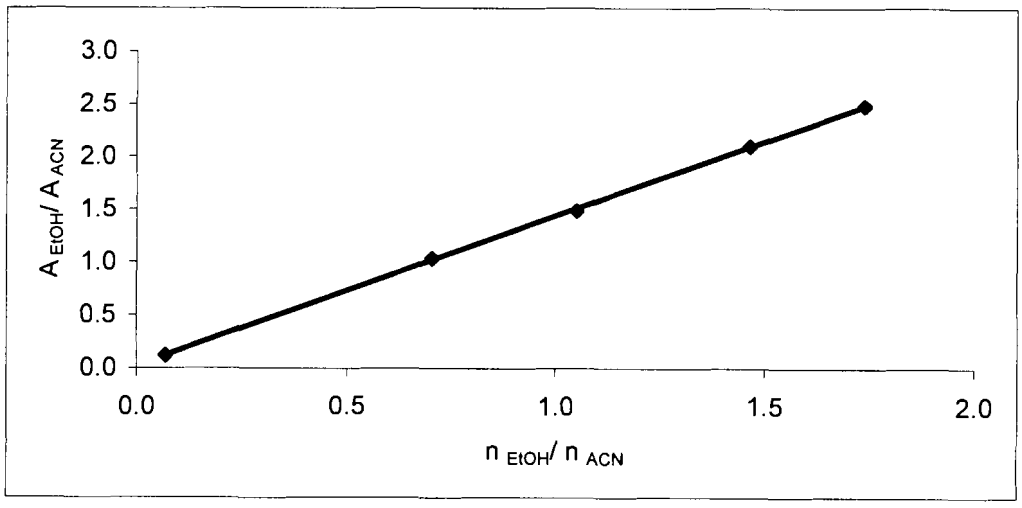


**Figure A.1: Calibration curve for ethanol-water mixtures**

## A.3 Determination of the composition from the calibration curve

The areas of the peaks, resulting from the analysis of a mixture from the GC in Figure A.2, was used to determine the composition of the mixture by converting the measured areas to mole fractions using the calibration curve in Figure A.1.

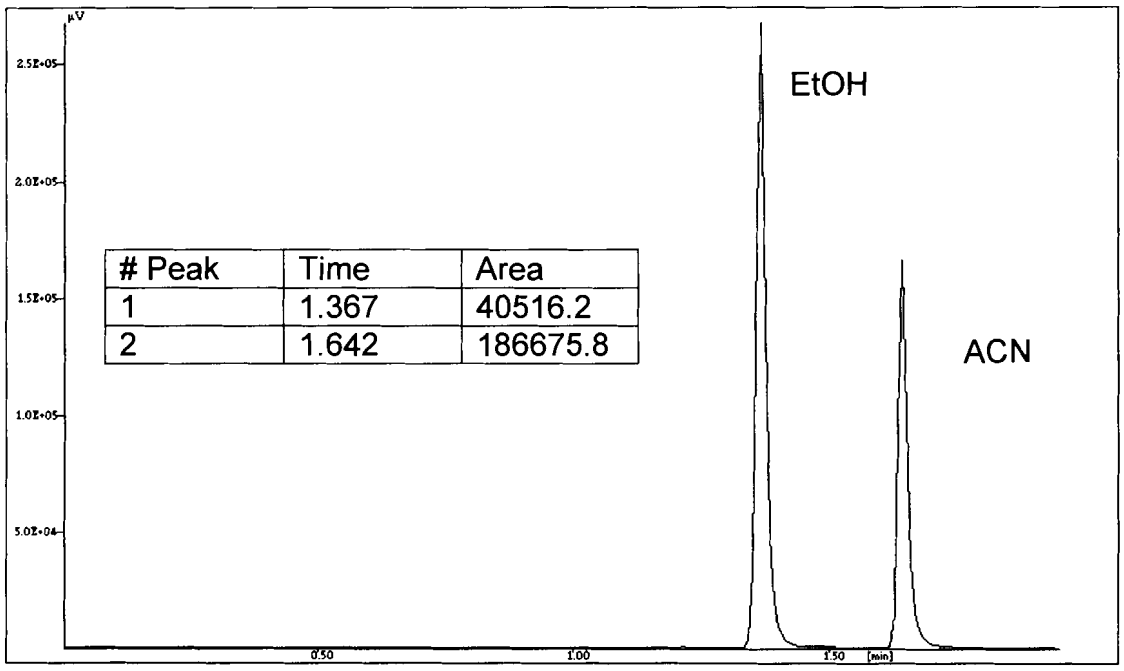


| # Peak | Time | Area |
|---|---|---|
| 1 | 1.367 | 40516.2 |
| 2 | 1.642 | 186675.8 |

**Figure A.2 Example of a GC chromatograph showing the peaks for ethanol and ACN**